ORGANIC CHEMISTRY







FRONTIERS

RESEARCH ARTICLE

View Article Online
View Journal | View Issue



Cite this: *Org. Chem. Front.*, 2021, **8**, 6561

Homolysis/mesolysis of alkoxyamines activated by chemical oxidation and photochemical-triggered radical reactions at room temperature†

Gérard Audran, *a Mitchell T. Blyth, b Michelle L. Coote, b Georg Gescheidt, c Micael Hardy, Jeffrey Havot, Maxence Holzritter, Samuel Jacoutot, Jean-Patrick Joly, *a Sylvain R. A. Marque, *b *a Tataye Moussounda Moussounda Koumba, Dmytro Neshchadin c and Enzo Vaiedelich

Alkoxyamines, which are connected with a phenol moiety by a (substituted) methylene bridge undergo homolytic cleavage upon chemical oxidation or a photo-induced hydrogen transfer. This selectively triggered reaction yields a nitroxide radical. In the presence of an excess of lead dioxide as the oxidant in *tert*-butylbenzene as solvent, spontaneous, instantaneous and almost quantitative generations of nitroxides from various alkoxyamines are observed at room temperature, which support activation energies for the cleavage lower than 100 kJ mol⁻¹. The rate and the amount of released nitroxide depend on the amount of "catalyst" and the structure of alkoxyamines.

Received 25th August 2021, Accepted 1st October 2021 DOI: 10.1039/d1qo01276b

rsc.li/frontiers-organic

Introduction

In the last decade, the concept of smart alkoxyamines has been developed.¹ These are highly stable alkoxyamines with half-lives of several hundred years, which can be selectively transformed into highly labile species with half-lives of seconds or minutes through chemical,²-5 photochemical⁶⁻⁹ or biochemical¹0,11</sup> events. Such alkoxyamines have interesting properties for potential applications in industry, *e.g.*, safe storage of initiators for radical polymerizations, ^{5,12} or in biology, *e.g.*, drugs for cancer or parasites. ^{10,11,13-18}

While the focus of these studies has been on triggering alkoxyamine *homolysis*, to form a nitroxide and carbon-centred radical, recently it has been shown that upon oxidation, through electrochemical^{19–23} or photoredox^{24,25} methods, alkoxyamines can spontaneously undergo *mesolytic* cleavage instead. Depending on the leaving group and other species present, this process can yield nitroxides and carbocations, or

alternatively oxoamoniums and carbon-centred radicals. In some cases, oxidation simply generates reactive intermediates capable of undergoing $S_{\rm N}2$ reactions with nucleophiles. These processes have been developed into successful alkylation methods in small molecule synthesis, 21,24 and likely have broader applications for the on-demand generation of carbon-centred radicals and cations. Moreover, it is thought that this mesolytic cleavage pathway may even be operative upon photochemical excitation of certain photoactive alkoxyamines. 26

To date, oxidative alkoxyamine cleavage has been achieved using either electrochemical or photoredox methods, but the use of simple chemical oxidation under mild conditions has not yet been reported. Indeed, while PbO2 has been shown to generate phenoxyl radicals from phenol-based anti-oxidants through proton-coupled electron transfer (PCET),²⁷ preliminary results with 3c show only very low conversion into nitroxide 3' using PbO2 as oxidant. Here, we report on the preparation phenol-based alkoxyamines 1a-5a,3e (Chart 1) and the benzyl protected homologues 1b-5b,3d (Chart 1). We have investigated their reaction pathways in t-BuPh as the solvent. At room temperature 1a-5a reacted with PbO2 affording almost quantitative conversions to the corresponding nitroxides. Kinetic investigations by EPR, product analysis, NMR/CIDNP, and DFT calculations of 1a-5a are used to unveil the pathways leading both to the decay of alkoxyamines and to the generation of nitroxides.

^aAix Marseille Univ, CNRS, ICR, UMR 7273, Case 551,

Avenue Escadrille Normandie-Niemen, 13397 Marseille Cedex 20, France.

E-mail: sylvain.marque@univ-amu.fr, g.audran@univ-amU.fr, jp.joly@live.fr

bResearch School of Chemistry, Australian National University, Canberra, ACT 2601,

Australia

^cInstitute of Physical and Theoretical Chemistry, TU Graz, Stremayrgasse 9/Z2, A-8010 Graz, Austria

[†] Electronic supplementary information (ESI) available: HRMS and NMR spectra of 1a,b-5a,b, 3d and $3e, pK_a$ determination of 4-vinylphenol, HPLC-ESI analysis of 3a and 3e in THF, and DFT calculations. See DOI: 10.1039/d1q001276b

Chart 1 Alkoxyamines and nitroxides investigated.

Results

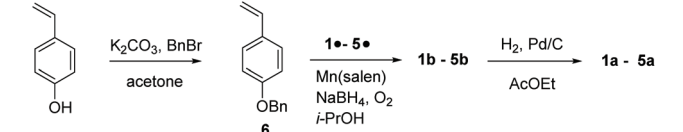
Synthesis

para-Vinyl phenol is protected by benzylation, ²⁸ ‡ to afford **6**, which is coupled with nitroxides **1**'-**5**' using the Mn(salen) method to yield **1b**-**5b**. ²⁹ § Then, **1b**-**5b** are deprotected using H₂ and the catalyst Pd/C²⁸ to yield **1a**-**5a** (Scheme 1).

The same procedures as displayed in Scheme 1 are applied for the preparation of **1d**, **3d**, and **3e** starting from *meta-*vinylphenol in 25%, 55%, and 74% yields, respectively.

Thermal homolysis

Effects of various substituents attached to the nitroxyl moiety on the homolysis rate constant k_d of the C-ON bond in alkoxyamines (Scheme 2) have been thoroughly investigated30-33 and it was shown that steric, polar and stabilization effects are strongly entangled.34,35 Noteworthy, for the thermal C-ON bond homolysis, differences of E_a of ca. 5-7 kJ mol⁻¹ between 1a and 3a, of ca. 5-7 kJ mol⁻¹ between 3a and 4a, of ca. 2-4 kJ mol⁻¹ between 3a and 5a are in the range of differences observed for analogue alkoxyamines. It means that the C-ON bond homolysis of 1a, 3a-5a is ruled by the polarity and bulkiness of the nitroxyl fragment, and stabilization of the released nitroxide as previously reported.34 Therefore, the thermal-triggered homolysis of 1a-5a occurs via the established mechanism³⁴ displayed in Scheme 2. Importantly, at high temperatures, in the presence of O2, the generation of alkyl radicals, peroxyl radicals, alkoxyl radicals and nitroxides do not alter the kinetics. Hence, the mechanism of homolysis via a selfcatalytic event in which the phenoxyl moiety would play the



Scheme 1 Preparation of 1a-5a.

Scheme 2 Geometrical parameters and orbital interactions expected in starting materials, TS, and products during the homolysis event.

role of radical scavenger, analogous to the Denisov cycle, ³⁶ is highly unlikely.

Effects of para-aryl substituent for 1-37 and 3-based38 alkoxyamines have been thoroughly investigated and linear free energy relationships (LFER) were observed for 1-based alkoxyamines³⁷ with the Hammett constant σ_p (ref. 39) and for 3-based alkoxyamines³⁸ with localized polar effect for parasubstituted phenyl groups $\sigma_{L,4-X-C_6H_4}$. Thus, E_a of 134.3 kJ mol^{-1} ¶ and 126.2 kJ mol^{-1} ∥ are estimated for 1a and 3a, respectively, in nice agreement with the experimental values reported in Table 1. Moreover, very similar values of E_a are expected for 1a and 1b** as well as for 3a and 3b†† agreeing with the values reported in Table 1. The trends in E_a observed for 1a-5a are also observed for 1b-5b. Hence, the C-ON bond homolysis for 1a,b-5a,b occur through TS exhibiting the same features:34 flattening at the N- and C-atoms of the C-ON moiety, rotation around the N-O bond to reach the dihedral angle (nitrogen lone pair NOC) at 0° ‡‡ and rotation around the C-aryl bond to reach the dihedral angle (OCaryl) at 90°. These geometric requirements favour the donating interactions $n_N \to \sigma^*_{O-C}$ of the nitrogen lone pair n_N into the C-O antibonding orbital σ^*_{O-C} , which in turn favours the donating interaction $\sigma_{O-C} \to \pi^*$ aryl of the O-C bonding orbital σ_{O-C} into the antibonding orbital π^* of the aryl moiety (Scheme 2).

Chemical oxidation

Taking into account the half-life times of 1a-5a at 25 °C ($t_{1/2} = 24$ days for 4a is the shortest, Table 1), these alkoxyamines are considered as stable during the 60 seconds of experimental time, *i.e.*, thermal homolysis of 0.1 mM of 4a affords 0.7 nM of

[‡]Disappointingly, all attempts for the preparation of 1a, 2a, and 5a using the procedure described in § failed.

[§] Alkoxyamines 3a and 4a are also prepared by the coupling of nitroxides 3' and 4' with the commercially available *para*-vinyl phenol using the procedure Mn (salen) (Scheme 1a).

 $[\]P\sigma_{\rm p,OH}$ = -0.37, see ref. 39, and equation in Fig. 2 in ref. 37.

 $[\]parallel \sigma_{\rm L,OH} = 0.24$ and $\sigma_{\rm R,OH}^0 = -049$, see ref. 40, and eqn (1) and (5a) in ref. 38.

^{**}It was assumed that $\sigma_{\rm p,OCH_2Ph} \approx \sigma_{\rm p,OEt}$ = -0.32, see ref. 39, and equation in Fig. 2 in ref. 37.

^{††}It was assumed that $\sigma_{L,4\text{-BnOC}_6H_4} \approx \sigma_{p,\text{OEt}}$, $\sigma_{L,\text{OEt}} = 0.28$ and $\sigma_{R,\text{OEt}}^0 = -044$, see ref. 40. and eqn (1) and (5a) in ref. 38.

 $[\]ddagger$ In general, this angle exhibit a deviation less than $\pm 20^{\circ}$ meaning that a very low activation entropic cost is expected.

Table 1 Homolysis rate constants kd for alkoxyamines (0.1 mM) 1a,d-5a,b, and 3d,e at various temperatures T in tert-butylbenzene as solvent and their corresponding activation energies $E_{\rm ar}$ homolysis rate constants $K_{\rm d}$ at 120 °C and half-life time $t_{1/2}$ at 25 °C

Alkoxyamines	<i>T</i> (°C)	$k_{\rm d} (10^{-3} {\rm s}^{-1})^a$	E_a^b (kJ mol ⁻¹)	$k'_{\rm d} (10^{-4} {\rm s}^{-1})^c$	$t_{1/2}^{d}$ (days)
1a	128	1.82	131.4	8.2	3613 (≈10 years)
2a	e	e	131.9^{f}	7.0	4416 (≈12 years)
3a	104	$0.66^{g,h}/1.4^{h,i}$	$126.8^{g,h}/124.4^{h,i}$	$34.2^{g,h}/70.4^{h,i}$	$547^{g,h}/219^{h,i}$
4a	80	$0.57^{g,h}/0.59^{h,i}$	$119.2^{g,h}/119.0^{h,i}$	$354.4^{g,h}/365.8^{h,i}$	$26^{g,h}/24^{h,i}$
5a	85	0.37	122.1	142.5	84
1b	138	3.80	132.2	0.65	5000 (≈14 years)
2b	130	1.68	132.3	6.2	5183 (≈14 years)
3b	122	$4.64^{g,h}/8.94^{h,i}$	$126.4^{g,h}/124.3^{h,i}$	$38.2^{g,h}/73.8^{h,i}$	$475^{g,h}/219^{h,i}$
4b	100	$2.79^{g,h}/3.37^{h,i}$	$121.0^{g,h}/120.4^{h,i}$	$202.9^{g,h}/242.7^{h,i}$	$55^{g,h}/40^{h,i}$
5 b	90	0.64	122.2	140.6	88
$1c^{j}$	_	_	133.0	5.0	6882 (≈19 years)
$3\mathbf{c}^{j}$	_	_	124.5	68.0	218
$4c^{j}$	_	_	121.3	181.0	61
$5c^{j}$	_	_	121.8	155.0	75
1d	120	0.39	133.9	3.9	9631 (≈26 years)
3d	100	$0.59^{g,h}/0.68^{h,i}$	$125.4^{g,h}/125.3^{h,i}$	$51.5^{g,h}/53.8^{h,i}$	$318^{g,h}/301^{h,i}$
3e	$100^{g,h}/90^{h,i}$	$0.76^{g,h}/0.27^{h,i}$	$125.0^{g,h}/124.87^{h,i}$	$59.1^{g,h}/62.9^{h,i}$	$265^{g,h}/245^{h,i}$

^a Values determined by EPR and using eqn (2). ^b Assuming an averaged frequency factor A = 2.4 × 10¹⁴ s⁻¹ (see ref. 34) and values of T and k given values defining an averaged frequency factor $A = 2.4 \times 10^{-8}$ (see fer. 34) and values of E_a given in fourth columns, respectively. ⁶ Values estimated at T = 120 °C assuming an averaged frequency factor $A = 2.4 \times 10^{14}$ s⁻¹ (see fer. 34) and values of E_a given in fourth columns. ^d Given at 25 °C and using values of E_a estimated as described in footnote c. ^e At $E_a = 130$ °C, $E_a = 13$ in chromatography. J See ref. 34.

nitroxide, below the threshold of detection of EPR at ca. 10 nM. PbO₂ is currently used to oxidize phenolic anti-oxidant into their corresponding phenoxyl radical for their detection by EPR. 42 Adding PbO₂ to 0.1 mM solution of 1a-5a at room temperature does not generate the EPR signal of the corresponding phenoxyl radical but an instantaneous raise of EPR signals corresponding to nitroxides 1'-5'. The intensity of the EPR signal of 1'-5' is PbO₂-concentration dependent affording bellshaped curves (Fig. 1). On the left-hand side of the top of bell curve, concentration in PbO₂ is too low for complete oxidation§§ whereas on the right-hand side, concentration in PbO2 is too large that it reacts with nitroxides. Nitroxides 4° and 5° are not displayed in Fig. 1 due to their too high reactivity with PbO₂ impeding any significant growth of the EPR signal whatever the concentrations in PbO₂. PbO₂-oxidation of 3e affords only 17% conversion in 3° as expected when less stabilized alkyl species is released from the *meta*-regioisomer of alkoxyamine.¶

Chemical activation via H-abstraction reaction

Organic Chemistry Frontiers

The use of PbO₂ as an oxidant generally also involves the transfer of protons. Since the reduction (of PbO₂) is accompanied by proton transfer, it formally corresponds to a H-atom transfer reaction. Accordingly, we have performed H-abstraction reactions induced by the photolysis of di-tertbutyl peroxide.

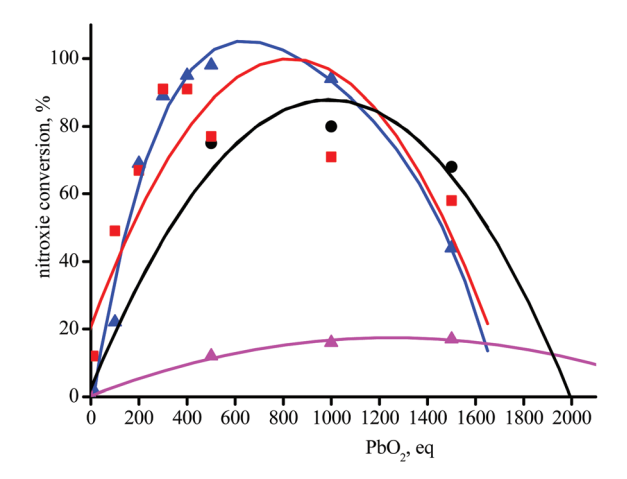


Fig. 1 Plots of nitroxide conversion vs. equivalents in PbO₂ with t-BuPh as solvent for 1' (red squares), 2' (black circles), and 3' (blue and magenta triangles) from 1a, 2a, 3a and 3e, respectively. Lines (second order polynomes) are for an easy reading of the trend.

The t-BuO radical (Scheme 3a) is able to primarily abstract the phenolic H-atom to generate a phenoxyl radical (Scheme 3d). 43 The latter can undergo fragmentation into a nitroxide and a methyne quinone like-product (Scheme 3e). Indeed, as soon as light is turned on, in a solution containing 3a and di-tertbutyl peroxide EPR signal of 3' raised affording around 80% conversion after a very long time (larger than 10 hours) of irradiation and for less than 5% (v/v) of di-tertbutyl peroxide (Table 2).

Disappointingly, a large amount of 40% conversion 3a into 3° is observed after 12 hours of UV-irradiation in the absence of peroxide. Thus, 3a as well as 1a and 2a are light sensitive. Nevertheless, the kinetics of generation of 3' are dramatically

^{§§} Several vigorous hand-shakings did not increase the EPR signal.

[¶]Stabilities of 1, 3-5 were investigated by EPR. 1 is stable in the presence of PbO2, 3' moderately stable, 4' and 5' decay quickly impeding all chances of detection when generated from their corresponding alkoxyamines. For 3' and 4', the signal of another radical carrying a phosphorylated moiety is observed but not identified. This species is unstable and decay quickly however, the side species of 3° is not obseverved during the oxidation of 3a.

Scheme 3 Elementary reactions involved during the generation of 3 under light-irradiation of a solution of 3a with (t-BuO)₂.

Table 2 Maximum conversion (%) and the corresponding time (t_{max}) for the generation of $1^{\circ}-3^{\circ}$ by the photolysis of tert-butylbenzene solutions (0.1 mM) of 1a-3a, and 3e in the presence (0%–10%) of di-tert-butyl peroxide t-Bu₂O₂ at room temperature

Alkoxyamines	tBu_2O_2 (%, v/v)	Equivalents ^a	Conversion ^b (%)	t _{max} c (min)
1a	0	0	24	300
2a	0	0	66	660
3a	0	0	49^d	720
3e	0	0	43^d	420
2a	0.1	66	63	720
3a	0.1	66	68	1260
1a	0.5	330	77	480
2a	0.5	330	67	540
3a	0.5	330	74	1020
3e	0.5	330	47	300
2a	1	660	62	240
3a	1	660	60	85
3a	5^e	3300	49	75
3a	10	6600	39	85

^a Density: d = 0.796. ^b Highest conversion observed. ^c Time for which the maximum conversion reported in the 4th column is observed. ^d When experiment was stopped. ^e When [3a] = 1 mM, no significant differences are observed both in conversion and in kinetics.

faster in the presence of more than 1% of $(tBuO)_2$ than in its absence (Fig. 2), that is, during the first 3 hours of irradiation, kinetics for the generation of 3' are the same for 0.1% in $(tBuO)_2$ and without whereas, in this time, amounts of 3' reached a plateau and completely decayed for amounts in $(tBuO)_2$ larger than 1% (Fig. 2). Notably, the plateau is reached faster for lower amounts of 3', *i.e.*, 30% released in 1000 s in 10% $(tBuO)_2$ versus 70% released in 10 hours for 0.5% in $(tBuO)_2$. This striking dependence on time for decomposition of 3a into nitroxide 3' is due to several competitive reactions involving 3', t-BuO', and side-products. Di-tertbutyl peroxide generates tert-butoxyl radicals under UV-irradiation (Scheme 3d). The latter reacts either by H-abstraction on the phenol moiety of 3a to generate a transient phenoxyl radical (Scheme 3b) or by β-fragmentation to afford acetone and methyl radicals (Scheme 3b). These methyl radicals

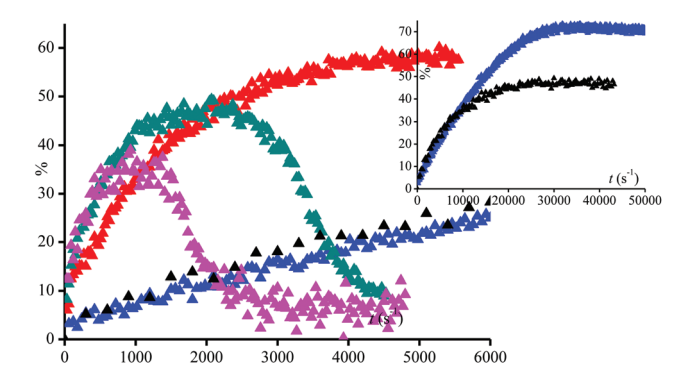


Fig. 2 UV-irradiation of **3a** (0.1 mM) in t-BuPh at 25 °C with various amounts (% v/v) of $(t-BuO)_2$ (\triangle) none, (\triangle) 0.5%, (\triangle) 1%, (\triangle) 5%, and (\triangle) 10%. Inset: Longer kinetics for conditions (\triangle) no $(t-BuO)_2$, and (\triangle) 0.5% $(t-BuO)_2$.

Chart 2 Potential product formed from 3a (10^{-2} M) upon the one-electron oxidation process by PbO₂ (500 eq.) in MeOH as solvent, at room temperature.

either react with 3' by the coupling reaction leading to the formation of stable alkoxyamines, and, hence, to the decay of 3' or they react with O₂ to afford oxidation products or some other radicals able to react with 3'. Consequently, several of these reactions depend dramatically on concentration of starting materials (tBu_2O_2 and 3a), of product (3' and possibly acetone and methine quinone like-compound), and also of intermediates such as t-BuO' and Me' radicals. Therefore, these differences in reactivity, account for the striking differences in conversion and in time to reach maximal conversion (Table 2).

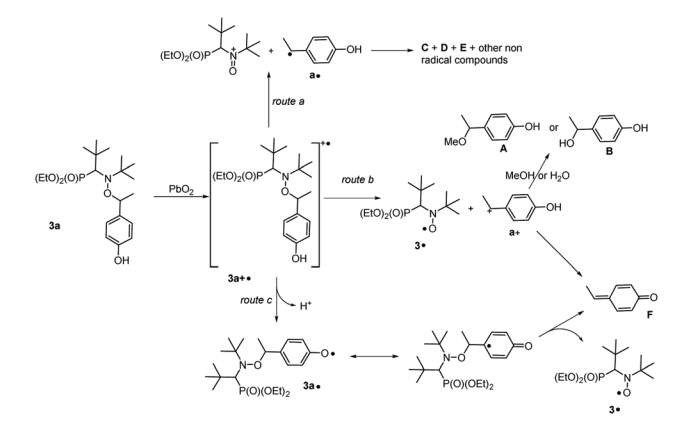
HPLC-ESI analysis

For HPLC experiments, chemical oxidation of **3a,e** (10^{-2} M) was performed in a 1:1 (v:v) MeOH/water mixture and afforded the same EPR results as in *t*-BuPh as solvent when 500 eq. PbO₂ were added. Authentic compounds displayed in Chart 2 are either prepared as described in literature (**A** and **B**) or purchased (**C** and **D**).|||***†† Compounds C-E are expected to be generated in the case of a mesolysis event

 $^{\| \|}$ Preparation of E and F is tedious, and as no unknown compounds is detected, no more efforts were devoted to their preparations.

^{***}Compounds issued from the degradation of 3e under chemical oxidation conditions were not prepared as the degradation processes are not clearly unveiled.

^{†††}Oxidations of **3a** and **3e** were performed in THF in the same conditions. In this case, the oxidation of **3a** afforded mainly **3*** and **B** as main products due to the traces of water in THF. For **3e**, results in THF were similar to those in MeOH.



Scheme 4 Different routes of decay of 3a+ describing HPLC observations reported in Table 3 and ESI.†

Table 3 Retention times in HPLC using UV detection (λ = 210 nm), mass analysis (ESI-MS), and mass balances for pure A-C, 3a, and 3b, and for 3a and 3e in the presence of 500 eq. of PbO2 in a MeOH/water (v:v 1:1) solvent mixture

	t^a	$m_{\rm e}/z^b$	$m_{\rm o}/z^b$	$n_{\rm a}^{c}$	n_3 · c	$n_{\rm o}^{\ c}$
A	11.2	153.2	121.2	n.a. ^d	n.a. ^d	1.0
C	12.5	121.2	121.2	n.a. ^d	n.a. ^d	1.0
3.	14.0	296.4	296.4	n.a. ^d	0.80^{e}	n.a. ^d
$3a^f$	15.6	416.2	416.2	0.56	n.a. ^d	n.a. ^d
	16.2			0.44		
$3e^g$	16.5	416.2	416.2	1.0	n.a. ^d	n.a. ^d
$3a + PbO_2$	11.1	n.a. ^d	121.2	n.a. ^d	n.a. ^d	0.51^{h}
	14.0		296.2	n.a. ^d	0.80	n.a. ^d
	15.6		416.2	0.05	n.a. ^d	n.a. ^d
	16.2		416.2	0.11	n.a. ^d	n.a. ^d
$3e + PbO_2$	14.0	n.a. ^d	296.2	n.a. ^d	0.07	n.a. ^d
	16.5		416.2	0.91	n.a. ^d	n.a. ^d

 a Retention time in min. b $m_{\rm e}/z$ and $m_{\rm o}/z$ are for the expected and observed masses by ESI-MS, respectively, in MeOH/H₂O (1:1 v:v), given at ± 0.1 u. c In 10^{-8} moles at ± 0.01 . $n_{\rm a}$, $n_{\rm 3}$, and $n_{\rm o}$ number of moles for alkoxyamines, 3°, and other molecules, respectively. d n.a.: not applicable. ^e As displayed in Fig. 3, 20% of impurities are detected. ^fMixture of 2 diastereoisomers. ^gOnly one diastereoisomers was available, h Amount of A.

releasing benzylic type radical and oxonium (route a in Scheme 4).

HPLC analysis of the decomposition of 3e (Table 3) displays only peaks corresponding to 3e (only 30% conversion) and to some traces of 3' (less than 10% in agreement with EPR results) meaning that the pathways of decomposition affording 3' are minor events (see section DFT calculations section and Fig. 7).

As displayed in Fig. 3, only 3a, 3° and A are observed for the decomposition of 3a in the presence of PbO2. No traces of other chemicals displayed in Chart 2 are detected. Mass balances (Table 3) for 3a (84% conversion) and 3' (80% conversion) agree with the EPR results. On the other hand, a clear discrepancy is observed in the mass balance for 3° (8 nmol against 5.1 nmol for A) meaning that most of the radical cation decomposes into nitroxide and benzylic-type carbo-

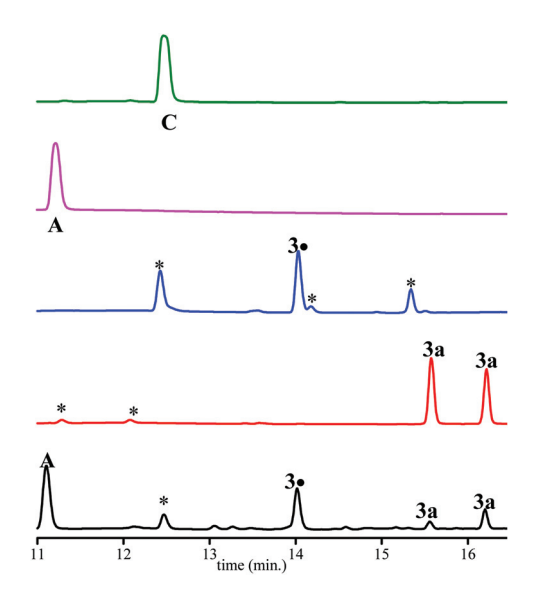


Fig. 3 HPLC signal of authentic compounds and of products for the chemical oxidation degradation of 3a. Concentrations are at 10⁻² M in MeOH/water (1:1 v:v). From top to bottom, HPLC traces of pure C (magenta), pure A (green); "pure" 3' (blue), pure 3a (red), and decomposition (black) of 3a in the presence of PbO2 (500 eq.).

cation a+ (route b, Scheme 4) which, is scavenged by MeOH to generate A provided the elimination reaction to afford C does not compete. The discrepancy observed is likely due to the occurrence of route c (Scheme 4) generating a phenoxyl radical 3a' which decomposes into nitroxide 3' and methine quinonetype compound F or to the loss of H+ from a+ to afford F. The latter cannot be detected under our experimental conditions.

Importantly, only 3a, 3', and C are detected by ESI-MS (Table 3). Indeed, for A and B, ESI detects only C, meaning that MeOH- or water-elimination occurs in the course of the ESI experiment. The HPLC mass balance shows that the decomposition of the radical cation of alkoxyamine 3a+ does not occur through route a (Scheme 4).

The same experiments have been performed with 3a in THF affording very similar results except that a+ is scavenged by traces of water in THF to yield B (see ESI table and figure†). When experiments are performed with 3e, similar results to those reported in Table 3 are observed (see ESI table†). Thus, all observations for 3a and 3e in MeOH/water mixture apply also to experiments performed in THF as solvent. It was assumed that the same reactivity would be expected for other phenol-based alkoxyamines not investigated by HPLC.

pK_a measurements

Due to solubility issues of 3a, THF: D₂O (v/v 1/1) mixture was used for ¹H NMR (Fig. 4). pK_a values of each diastereoisomer of 3a (Fig. 5) are given as 12.3 (±0.02) and 12.8 (±0.05) using eqn (1).⁴⁴ p K_a Values of paravinylphenol are measured as 12.0 when recorded in the same conditions (see ESI†).

$$\delta_{\mathrm{pH}} = \delta + \frac{\delta_{\mathrm{H}^{+}} - \delta}{1 + 10^{\mathrm{p}K_{\mathrm{a}} - \mathrm{pH}}} \tag{1}$$

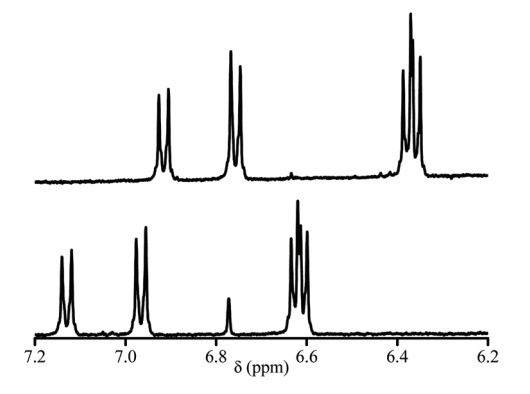


Fig. 4 400 MHz ¹H NMR signal of the aromatic zone at pH = 13. (Top) and at pH = 1.3 (bottom) of 3a in THF.

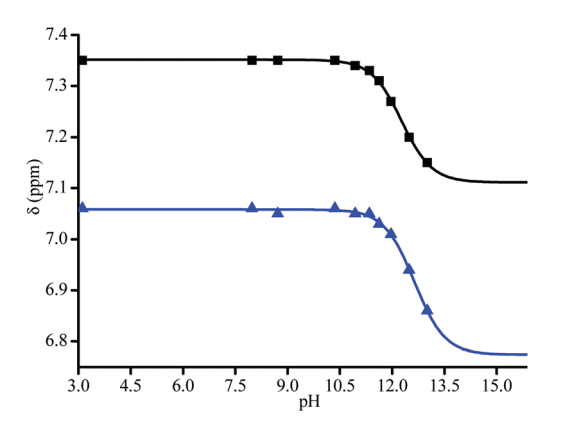


Fig. 5 pH curves for diastereoisomers of 3a (▲ and ■) by 2 peaks in the aromatic zone (see Fig. 4). Data were fitted with egn (1).

CIDNP experiments

The experiments described above indicate that the formal abstraction of the phenolic H atom induces the formation of the nitroxyl radical. To shed light on the mechanism of the underlying reaction sequence at a µs time scale, we performed photo-induced TR-CIDNP (Time-Resolved Chemically Induced Dynamic Nuclear Polarization) experiments. 45,46 As an example, we present the results obtained with 3a (see ESI† for more derivatives). We have used benzophenone (BP) as the photo-activated hydrogen acceptor. It reacts in an analogous way as the t-BuO' radical (see above Scheme 3d) and can be conveniently activated at 366 nm (NdYAG laser, used in our CIDNP system). We have utilized this approach to successfully study various H-transfer reactions. 47,48

In the CIDNP experiment, free radical pairs are generated thermally or photochemically inside the strong magnetic field of the NMR magnet. At the time scale of the CIDNP experiment, the primary radicals undergo reactions, which are spin selective. This leads to a non-Boltzmann population of magnetic energy levels and manifests itself in NMR signals with "unusual" intensities, i.e. enhanced absorption or emission (enhancement factors up to 10⁵) when the corresponding products are formed via radical pairs. The intensities of these

Scheme 5 generation of 3' during the irradiation (NdYAG laser, 355 nm, 8 ns) of benzophenone (3 mM) in the presence of 3a (1 mM) at 25 °C in acetonitrile-d₃/D₂O.

polarized signals (of the products) provide information about the isotropic hyperfine coupling constants in the short-lived radical intermediates. To produce primary radical pairs, we used the photo-induced (NdYAG laser, 355 nm, 8 ns) reaction of the triplet-excited state of BP ($^{3}*BP$) with alkoxyamine in acetonitrile-d₃/D₂O (Scheme 5). Primarily, ³*BP should abstract the phenolic hydrogen^{49,50} and the corresponding follow-up products are observed in CIDNP spectrum with the chemical shifts representing the products and the polarized line intensities indicating the intermediate radicals (Scheme 5). As an example, the ¹H NMR and CIDNP spectra obtained from 3a together with assignments of selected lines are shown in Fig. 7. The most prominent polarizations in the CIDNP spectrum (7.7 ppm and 8-8.2 ppm) can be attributed to the reversible hydrogen transfer from BPH' to 3a' re-generating BP and 3a (Scheme 5). This is in concert with an intermediate phenoxyl radical where the predominant spin population is located on the phenyl ring of 3a in agreement with B3LYP/ TZVP calculations. 51,52 Clearly, an electron transfer producing a basically nitrogen centred radical cation from 3a to 3*BP, would have produced an entirely different polarization pattern than that observed in our experiment (see ESI† for the com-

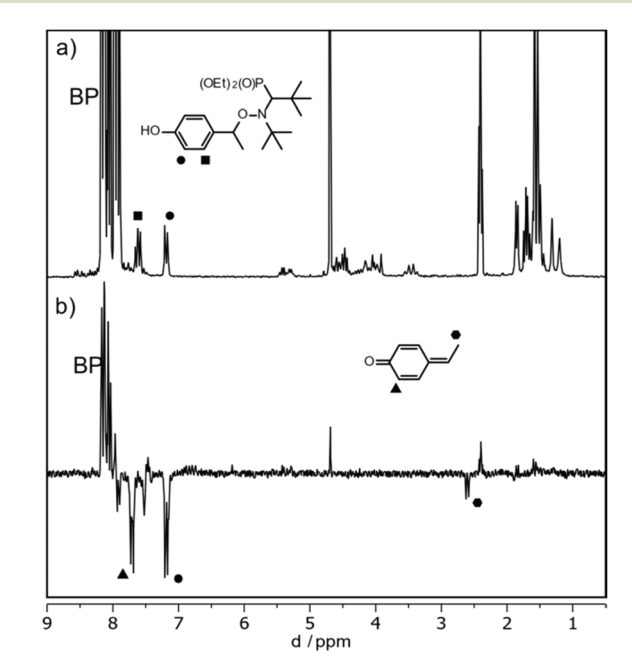


Fig. 6 ¹H NMR (a) and (b) CIDNP spectrum of 3a and BP in Acetonitrile d_3/D_2O recorded 2 μs after the laser flash (355 nm, 8 ns).

parison with additional radicals). The remaining polarizations at 2.55 ppm (doublet) and 7.7 ppm (doublet) can be assigned to a methyne quinone like-product F (Chart 2 and Fig. 6) formed via the homolytic cleavage of the C-O bond in 3a. This intermediate is too short lived to be detected in the steady-state NMR taken after the CIDNP experiment. The fragmentation of 3a' yielding nitroxyl radical 3' is confirmed by the detection of the corresponding EPR spectrum taken from the NMR tube after accomplishing the NMR experiment.

For derivative 3b, in which the phenolic hydrogen is replaced by the benzyl group, the fragmentation reaction cannot be established by CIDNP (see ESI†); moreover, weak EPR signal is detected. This clearly indicates that the abstraction of the phenolic hydrogen is crucial for the formation of nitroxyl radical 3'.

DFT calculations

We have performed calculations (M06-2X/6-31+G(d,p) level of theory)⁵³ for radical cations and phenoxyl radicals based on parent 3a and 3e. In Fig. 7, we have displayed the most exergonic (or the lowest endergonic) pathways for the decomposition of 3a and 3e under oxidative conditions (see the ESI† for pathways with highly endergonic ΔG values). For 3a there are three pathways starting from the same radical cation 3a+ as intermediate which are preferable. One pathway (Path 3a(I)) involves the cleavage of the N-O bond and the formation of an aminium

cation N+ and alkoxyl radical O' ($\Delta G = -51 \text{ kJ mol}^{-1}$). The second radical-cation-based process produces the desired nitroxide together with benzyl cation a+ (Path 3a(II), $\Delta G = -27$ kJ mol^{-1}). The third one, the reaction *via* neutral phenoxyl radical 3a provides nitroxide 3 and 4-ethylidenecyclohexa-2,5-dien-1one F (Path 3a(III), $\Delta G = -49 \text{ kJ mol}^{-1}$). The calculations predict two likely reactions for 3e and both are based on radical cation precursors 3e+*: one being analogous to Path 3a(I) and vielding aminium cation N+ and alkoxyl radical O' (Path 3e(I), $\Delta G =$ -55 kJ mol⁻¹); the second resembling Path 3a(II) giving the desired nitroxide 3° and benzyl cation e+ (Path 3e(II), $\Delta G = +9$ kJ mol⁻¹). In contrast to 3a, paths 3e(III) is disregarded due to its too high value of ΔG , *i.e.*, 72 kJ mol⁻¹. As delineated in Fig. 7, for both the radical cations 3a+ and 3e+ issued from the oxidation of 3a and 3e, respectively, there is a connection between oxidation and HAT routes as the radical cation affords phenoxyl radical by loss of proton. Taking into account EPR, CIDNP, and HPLC results, paths 3a(I) and 3e(III) are disregarded.

Discussion

Chemical activation via H-abstraction reaction

The generation of 3a' through H-abstraction by t-BuO' radicals and its β-fragmentation into 3° and F, which are entangled with (several) light-initiated reactions, are nicely confirmed by CIDNP experiments by using benzophenone as radical

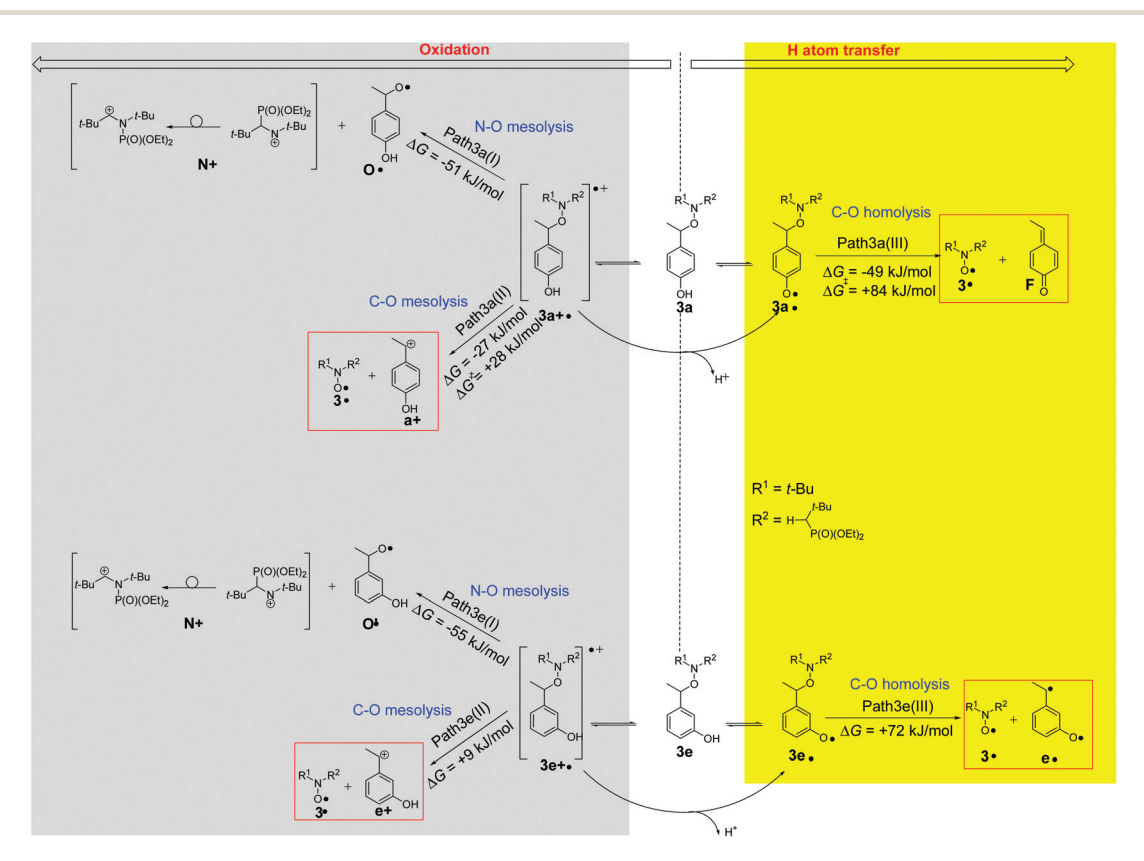


Fig. 7 Selected (preferred) pathways of decomposition radicals based on 3a and 3e according to M06-2X/6-31+G(d,p) calculations. Reactions leading to the release of nitroxyl radicals are marked with red boxes.

initiator. Moreover, DFT calculations support the occurrence of Path3a(III) which exhibit clear negative value of ΔG with ΔG^{\ddagger} lower than 90 kJ mol⁻¹ as expected for the occurrence of spontaneous and instantaneous reactions. As the same kinetic trends are observed (Table 2) for **1a**, and **2a**, it is assumed that the observations for **3a** apply to these also.

Activation by electron transfer event

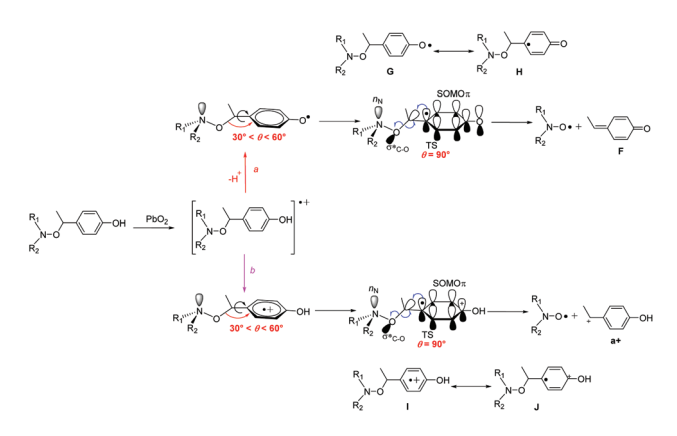
Research Article

Previous studies have examined the behaviour of amoniumyl radical cations generated upon oxidation of alkoxyamines by electrochemical $^{19-23}$ or photoredox 24 methods. Depending on the leaving group and co-reactants present, the oxidation can either be (a) reversible, or lead to mesolytic cleavage of either the (b) CO–N bond to form aminyl radicals, or cleavage of the C–ON to form either (c) an oxoamonium and carbon-centred radical or (d) a nitroxide and carbocation. Alternatively, cleavage can occur via (e) S_N2 -type reactions with nucleophiles, which may include trace water, the solvent or electrolyte. Importantly, in the case of 1c, only route (d) has been observed experimentally in anhydrous solvents, 19,23 and one would expect analogous behaviour for 3c, given that the leaving group is identical.

Whatever the amounts of PbO_2 added to a solution of 3c in t-BuPh, less than 4% of signal is detected by EPR. When the same experiments are performed with 3c, less than 20% of 3 are detected by EPR (Fig. 1) in agreement with HPLC measurements (Table 3), and calculations meaning that path(II) (path3c(II) in Fig. 7) is a minor event in the generation of 3 by chemical oxidation process when the released benzylic-cation is not stabilized. This also holds for other alkoxyamines investigated in this article (*vide infra*).

DFT calculations on the homolysis routes (Fig. 7) show only two relevant processes of fragmentations (other are displayed as ESI†): (i) mesolysis of the C–ON bond in 3a+' affording nitroxide 3' and benzyl-type carbocation a+ ($\Delta G_b = -27 \text{ kJ mol}^{-1}$, and $\Delta G^{\ddagger} = 28 \text{ kJ mol}^{-1}$, Path3a(II) in Fig. 7); and (ii) via proton release from 3a+' to generate phenoxyl radical 3a'‡‡‡ which collapses into nitroxide 3' and methine-quinone type compound F ($\Delta G_c = -49 \text{ kJ mol}^{-1}$, route c in Scheme 4 and Path3a (III) in Fig. 7), *i.e.* Proton-Coupled Electron Transfer (PCET)^{27,54} followed by a β -fragmentation event. The mesolysis of the C–ON affording oxonium and stabilized styryl-type radical a' (see ESI†), is disregarded due to both strongly disfavoured ΔG value ($\Delta G_a = 75 \text{ kJ mol}^{-1}$, see ESI†) and an almost quantitative generation of 3'.

Indeed, DFT calculated negative ΔG values and ΔG^{\ddagger} values lower than 100 kJ mol⁻¹ confirm the spontaneous and instantaneous generation of 3°. Moreover, the lower activation ΔG^{\ddagger} for path3a(II) ($\Delta G_b^{\ddagger} = 28 \text{ kJ mol}^{-1}$) than for path3a(III) ($\Delta G_c^{\ddagger} = 84 \text{ kJ mol}^{-1}$) in Fig. 7 denotes a favoured path3a(II) over path3a(III) as highlighted by the mass balance in HPLC (Table 3).



Scheme 6 Generation of nitroxide from alkoxyamine through a PCET process coupled with the β -fragmentation of phenoxyl radical (route a) and the mesolysis of radical cation (route b), and geometrical parameters and orbital interaction at their respective TS.

The quantitative generation of 1° and 2° is observed upon addition of PbO₂ to a solution of 1a and 2a, meaning that comments done for 3a hold.

Addition of PbO_2 to 4a and 5a does not generate significant amounts of the corresponding nitroxides 4° and 5° due to their low stability in the experimental conditions. ¶¶ Nevertheless, it is assumed that the same chemistry as described for 3a holds for 4a and 5a.

Impact on the fragmentation pathway

It has to be mentioned that, whatever the experimental conditions, the phenoxyl radical and radical cation are not detected by EPR meaning a very fast decomposition into the nitroxide. Thus, the generation of nitroxide cannot occur as described in Scheme 2 in which flattening at N- and C-atoms is required. Recent DFT calculations showed that C-ON bond homolysis is controlled by two geometrical requirements (Scheme 2): (i) flattening at N- and C-atoms, and (ii) dihedral angle θ (OCaryl) close to 90° and dihedral angle θ_1 (n_N NOC) close to 0°. It was also shown that alkoxyamines exhibiting angle θ close to 90° and θ_1 close to 0° are stable at room temperature meaning that the flattening at C- and N-atoms are the key events which must occur during the raise of temperature when homolysis is performed. Thus, two pathways of decay are offered to the radical cation: route (a) for which the radical cation collapses into nitroxide and benzylic-type cation and route (b) which correspond to the release of phenoxyl radical. Interestingly, both routes exhibit strong similarities for stereoelectronic interactions at TS (Scheme 6), i.e., mesomeric forms H of phenoxyl radical G and J of radical cation I display a significant spin population at the position ipso. Such forms H/J favour the rotation around the C-aryl bond to shift θ angle from 60°§§§ to 90° (see TS section in ESI†) aiming to favour hyperconjugative interaction SOMO $\pi \rightarrow \sigma^*_{C-O}$ between the

§§§ For most 3-based alkoxyamines carrying an aryl moiety on the alkyl fragment, the dihedral angle θ is close to 60° .

 $[\]ddagger$ Noteworthily, the addition of PbO₂ on molecules exhibiting phenol moieties is well known to generate phenoxyl radical through a Proton-Coupled Electron Transfer (PCET, see ref. 54 and 27) *via* the generation of radical cation and loss of proton to provide a phenoxyl radical.

SOMO of π -type and the antibonding orbital σ^*_{C-O} of the C–O bond. Such an interaction at TS favours undoubtedly the β -fragmentation event of the O–C bond affording two highly stabilized molecules: a nitroxide and a conjugated keto diene despite aromaticity is lost for the fragmentation of phenoxyl radical, and a nitroxide and a benzylic-type cation for the mesolysis of the radical cation. In such a process involving early TS, *i.e.*, reactant-like TS, neither the unfavoured N-flattening event nor the N–O bond rotation occur leading to a room temperature spontaneously and instantaneously thermodynamically-driven fragmentation.

Our experimental observations and the computational results indicate that the very efficient production of the nitroxide (e.g. 3') is based either on the primary generation of a phenoxyl radical via hydrogen abstraction or PCET (which cannot be distinguished at the time scale of our experiments) or the mesolysis of the corresponding radical cation. The main prerequisite for an efficient reaction, however, is that an alkyl fragment carrying a p-phenolic moiety as exemplified with 1a-5a. Here the release of the nitroxide can be either triggered thermally by PbO₂ or by photo-induced reactions. Thus, the caged nitroxides introduced in this work have the potential of being applied in biology and polymer chemistry (e.g., as selectively activable labels). It is likely that the scope of (photo)oxidants can be enhanced.

Experimental

Synthetic procedures

Solvents and reactants for the preparation of alkoxyamines were used as received. Routine reaction monitoring was performed using silica gel 60 F254 TLC plates; spots were visualized upon exposure to UV light and a phosphomolybdic acid solution in EtOH, followed by heating. Purifications were performed on Reveleris® X2 Flash System BUCHI Switzerland. Cartouches flash Reveleris® et GraceResolv™: silica 40 µm. ¹H, ¹³C, and ³¹P NMR spectra were recorded in CDCl₃ on a 300 or 400 MHz spectrometer. Chemical shifts (δ) in ppm were reported using residual nondeuterated solvents as internal references for ¹H and ¹³C NMR spectra, and 85% H₃PO₄ for ³¹P-NMR spectra. High-resolution mass spectra (HRMS) were performed on a SYNAPT G2 HDMS (Waters) spectrometer equipped with a pneumatically assisted atmospheric pressure ionization source (API). Positive mode electrospray ionization was used on samples: electrospray voltage (ISV): 2800 V; opening voltage (OR): 20 V; nebulizer gas pressure (nitrogen): 800 L h⁻¹. Low resolution mass spectra were recorded on the ion trap AB SCIEX 3200 QTRAP equipped with an electrospray source. The parent ion $[M + H]^+$ is quoted.

Benzylation of vinylphenol. To a stirred solution of vinylphenol (10% w/w in propylene glycol, 5.0 g, 4.16 mmol, 1 eq.) in acetone (70 mL), was added K_2CO_3 (3.8 g, 27.04 mmol, 6.5 eq.), then benzylbromide (2.3 g, 13.31 mmol, 3.2 eq.). The reaction was stirred at room temperature for 24 h. After this

time, the solvent was evaporated, diluted with EtOAc (80 mL) and 3 M aq. HCl was carefully added. The layers were separated, and the organic phase was washed with water, brine and dried over MgSO₄. After concentration under reduced pressure, the residue was purified by column chromatography (petroleum ether/EtOAc; gradient: 100% to 80%) to afford 6 (743 mg, 85%).

General procedure for the preparation of 1b–5b. To a stirred solution of Salen ligand (0.15 eq.) in i-PrOH was added MnCl₂ (0.15 eq.) in an open flask. After 30 minutes of stirring at room temperature, a solution of nitroxyde 1'–5' (1 eq.) and 4-vinylbenzylphenol 6 (1.1 eq.) in i-PrOH was added first, then solid NaBH₄ (5 eq.) in small portions. The resulting suspension was stirred at room temperature for 7 h. It was then diluted with EtOAc (100 mL) and 1 M aq. HCl was carefully added. Solid NaHCO₃ was then added until neutralization. The layers were separated, and the organic phase was washed with water, brine and dried over MgSO₄. After concentration under reduced pressure, the residue was purified by column chromatography (petroleum ether/EtOAc) to afford the corresponding alkoxyamines 1b–5b.

General procedure of hydrogenation for the preparation of 1a-5a. To a stirred solution of benzylated alkoxyamine 1b-5b (1 eq.) in EtOAc was added Pd/C (10% w/w) with a flow of hydrogen for 30 minutes. After a complete consumption of starting material monitored by TLC, the solution was filtered on Celite. It was then concentrated under reduced pressure and the residue was purified, if necessary, by column chromatography (petroleum ether/EtOAc) to afford the corresponding alkoxyamines 1a-5a.

Synthesis of 1-(1-(4-(benzyloxy)phenyl)ethoxy)-2,2,6,6-tetramethylpiperidine (1b). Alkoxyamines 1b was prepared according to the general procedure using Salen ligand (87 mg, 0.324 mmol, 0.15 eq.), MnCl₂ (64 mg, 0.324 mmol, 0.15 eq.), 1 (338 mg, 2.161 mmol, 1.0 eq.), 4-vinylbenzylphenol (500 mg, 2.378 mmol, 1.1 eq.) and NaBH₄ (409 mg, 10.805 mmol, 5.0 eq.). Alkoxyamine was purified by automatic flash column chromatography (petroleum ether/EtOAc; gradient: 100% to 80%) to afford 1b (516 mg, 65%), white solid; m.p.: 100 °C; $R_{\rm f} = 0.75 \; (EP/EtOAc \; 96:4); \; ^{1}H \; NMR \; (300 \; MHz, \; CDCl_{3})$ δ 7.49–7.30 (m, 5H), 7.25 (d, J = 8.7 Hz, 2H), 6.93 (d, J = 8.7 Hz, 2H), 5.06 (s, 2H), 4.75 (q, J = 6.7 Hz, 1H), 1.47 (d, J = 6.7 Hz, 3H), 1.45-0.99 (m, 15H), 0.68 (s, 3H). ¹³C NMR (75 MHz, CDCl₃) δ 157.7 (C), 138.3 (C), 137.2 (C), 128.5 (2 × CH), 127.9 (CH), 127.8 (2 × CH), 127.5 (2 × CH), 114.3 (2 × CH), 82.4 (CH), 70.0 (CH₂), 59.7 (2 × C), 40.3 (2 × CH₂), 34.4 (2 × CH₃), 23.2 (CH₃), 20.2 (2 × CH₃), 17.2 (CH₂). HRMS m/z (ESI) Calcd for $C_{24}H_{34}NO_2^+[M+H]^+$ 368.2584 Found: 368.2581.

Synthesis of 1-(1-(4-(benzyloxy)phenyl)ethoxy)-2,2,5,5-tetramethylpyrrolidine (2b). Alkoxyamines 2b was prepared according to the general procedure using Salen ligand (85 mg, 0.316 mmol, 0.15 eq.), $MnCl_2$ (63 mg, 0.316 mmol, 0.15 eq.), 2 (300 mg, 2.110 mmol, 1.0 eq.), 4-vinylbenzylphenol (532 mg, 2.532 mmol, 1.2 eq.) and NaBH₄ (399 mg, 10.550 mmol, 5.0 eq.). Alkoxyamine was purified by automatic flash column chromatography (petroleum ether/EtOAc; gradient: 100% to

80%) to afford **2b** (566 mg, 76%), white solid; m.p.: 59 °C; $R_{\rm f}$ = 0.73 (EP/EtOAc 96:4); ¹H NMR (300 MHz, CDCl₃) δ 7.51–7.35 (m, 5H), 7.31 (d, J = 8.7 Hz, 2H), 6.98 (d, J = 8.7 Hz, 2H), 5.09 (s, 2H), 4.67 (q, J = 6.6 Hz, 1H), 1.62–145 (m, 4H), 1.50 (d, J = 6.6 Hz, 3H), 1.31 (s, 3H), 1.21 (s, 3H), 1.08 (s, 3H), 0.73 (s, 3H). ¹³C NMR (75 MHz, CDCl₃) δ 158.0 (C), 137.5 (C), 137.2 (C), 128.5 (2 × CH), 128.2 (2 × CH), 127.8 (CH), 127.4 (2 × CH), 114.2 (2 × CH), 81.6 (CH), 70.0 (CH₂), 64.2 (C), 63.2 (C), 36.1 (CH₂), 35.4 (CH₂), 31.2 (CH₃), 31.1 (CH₃), 24.3 (CH₃), 22.8 (CH₃), 22.1 (CH₃). HRMS m/z (ESI) Calcd for C₂₃H₃₂NO₂ ⁺ [M + H]⁺ 354.2428 Found: 354.2422.

Synthesis of diethyl(1-((1-(4-(benzyloxy)phenyl)ethoxy) (tert-butyl)amino)-2,2-dimethylpropyl)phosphonate Alkoxyamines 3b was prepared according to the general procedure using Salen ligand (137 mg, 0.510 mmol, 0.15 eq.), MnCl₂ (100 mg, 0.510 mmol, 0.15 eq.), 3° (1.0 g, 3.401 mmol, 1.0 eq.), 4-vinylbenzylphenol (858 mg, 4.081 mmol, 1.2 eq.) and NaBH₄ (643 mg, 17.005 mmol, 5.0 eq.). The solvent was evaporated to give the crude product as mixture of diastereoisomers. The diastereoisomers were separated by automatic flash column chromatography (petroleum ether/EtOAc; gradient: 100% to 50%) to afford (RR/SS)-3b (600 mg, 35%) and (RS/ SR)-3b (548 mg, 32%). (RR/SS)-3b; pale yellow oil; $R_f = 0.54$ (EP/ EtOAc 4:1); ¹H NMR (400 MHz, CDCl₃) δ 7.46-7.31 (m, 5H), 7.23 (d, J = 8.6 Hz, 2H), 6.91 (d, J = 8.7 Hz, 2H), 5.05 (s, 2H), 4.96 (q, J = 6.7 Hz, 1H), 4.38-4.31 (m, 1H), 4.23-4.04 (m, 2H),4.04-3.89 (m, 1H), 3.35 (d, J_{H-P} = 26.2 Hz, 1H), 1.59 (d, J = 6.7 Hz, 3H), 1.35-1.30 (m, 6H), 1.25 (s, 9H), 0.85 (s, 9H). 31 P NMR (121 MHz, CDCl₃) δ 25.82. 13 C NMR (75 MHz, Acetone) δ 152.1 (C), 132.0 (C), 131.3(C), 122.8 (4 × CH), 122.1 (CH), 121.7 (2 × CH), 108.5 (2 × CH), 78.4 (CH), 64.2 (CH₂), 64.2 (d, J_{C-P} = 138.9 Hz, CH), 55.8 (d, J_{C-P} = 6.5 Hz, CH₂), 55.4 (C), 53.1 (d, J_{C-P} = 8.2 Hz, CH₂), 29.8 (d, J_{C-P} = 5.6 Hz, C), 24.5 $(d, J_{C-P} = 6.1 \text{ Hz}, 3 \times CH_3), 22.8 (3 \times CH_3), 17.8 (CH_3), 11.0 (d,$ $J_{C-P} = 5.7 \text{ Hz}, CH_3$, 10.5 (d, $J_{C-P} = 6.6 \text{ Hz}, CH_3$). HRMS m/z(ESI) Calcd for $C_{28}H_{45}NO_5P^+$ [M + H]⁺ 505.3030 Found: 505.3031. (RS/SR)-3b; pale yellow oil; $R_f = 0.67$ (EP/EtOAc 4:1); ¹H NMR (400 MHz, CDCl₃) δ 7.31 (d, J = 8.7 Hz, 2H), 7.35–7.18 (m, 5H), 6.81 (d, J = 8.7 Hz, 2H), 5.13 (q, J = 6.6 Hz, 1H), 4.95 (s, 2H), 4.08-3.84 (m, 1H), 3.85-3.69 (m, 1H), 3.46-3.30 (m, 1H), 3.32 (d, J_{H-P} = 26.0 Hz, 1H), 3.26–3.10 (m, 1H), 1.45 (d, J = 6.6 Hz, 3H), 1.16 (t, J = 7.1 Hz, 3H), 1.13 (s, 9H), 1.11 (s, 9H), 0.81 (t, J = 7.1 Hz, 3H). ³¹P NMR (121 MHz, CDCl₃) δ 24.62. ¹³C NMR (101 MHz, CDCl₃) δ 158.0 (C), 137.1 (C), 135.7 (C), 129.1 (2 × CH), 128.4 (2 × CH), 127.7 (CH), 127.3 (2 × CH), 114.2 (2 × CH), 77.7 (CH), 70.1 (d, J_{C-P} = 139.3 Hz, CH), 69.8 (CH₂), 61.6 $(d, J_{C-P} = 6.3 \text{ Hz}, CH_2), 61.1 (C), 58.5 (d, J_{C-P} = 7.5 \text{ Hz}, CH_2),$ 35.3 (d, J_{C-P} = 5.1 Hz, C), 30.6 (d, J_{C-P} = 6.0 Hz, 3 × CH₃), 28.1 $(3 \times CH_3)$, 20.9 (CH₃), 16.3 (d, $J_{C-P} = 5.9$ Hz, CH₃), 16.1 (d, $J_{\text{C-P}} = 6.9 \text{ Hz}$, CH₃). HRMS m/z (ESI) Calcd for $C_{28}H_{45}NO_5P^+$ [M + H]⁺ 505.3030 Found: 505.3031

Synthesis of diethyl(1-((1-(4-(benzyloxy)phenyl)ethoxy) (1-hydroxy-2-methylpropan-2-yl)amino)-2,2-dimethylpropyl) phosphonate (4b). Alkoxyamines 4b was prepared according to the general procedure using Salen ligand (130 mg, 0.483 mmol, 0.15 eq.), MnCl₂ (95 mg, 0.483 mmol, 0.15 eq.), 4

(1.0 g, 3.226 mmol, 1.0 eq.), 4-vinylbenzylphenol (814 mg, 3.871 mmol, 1.2 eq.) and NaBH₄ (611 mg, 16.130 mmol, 5.0 eq.). The solvent was evaporated to give the crude product as mixture of diastereoisomers. The diastereoisomers were separated by automatic flash column chromatography (petroleum ether/EtOAc; gradient: 100% to 40%) to afford (RR/SS)-4b (521 mg, 31%) and (RS/SR)-4b (454 mg, 27%). (RR/SS)-4b; white solid; m.p.: 65 °C; $R_f = 0.66$ (EP/EtOAc 7:3); ¹H NMR (400 MHz, CDCl3) δ 7.63–7.42 (m, 2H), 7.42–7.36 (m, 2H), 7.34 (d, J = 7.2 Hz, 1H), 7.29 (d, J = 8.6 Hz, 2H), 6.95 (d, J = 8.7 Hz,2H), 5.06 (s, 2H), 4.94 (q, J = 6.6 Hz, 1H), 4.29 (m, 1H), 4.23-3.92 (m, 3H), 3.67 (d, J_{H-P} = 26.7 Hz, 1H), 3.46 (d, J = 12.0 Hz, 1H), 3.09 (d, J = 12.0 Hz, 1H), 1.56 (d, J = 6.6 Hz, 3H), 1.37(t, J = 7.1 Hz, 6H), 1.24 (s, 9H), 1.05 (s, 3H), 0.80 (s, 3H).NMR (121 MHz, CDCl₃) δ 26.89. ¹³C NMR (75 MHz, CDCl₃) δ 158.0 (C), 137.1 (C), 136.9 (C), 128.5 (2 × CH), 128.0 (2 × CH), 127.8 (CH), 127.5 (2 × CH), 114.4 (2 × CH), 83.85 (CH), 69.8 (CH_2) , 69.3 (d, J_{C-P} = 139.3 Hz, CH), 67.4 (CH₂), 64.7 (C), 61.7 (d, $J_{C-P} = 6.3 \text{ Hz}$, CH_2), 60.3 (d, $J_{C-P} = 6.3 \text{ Hz}$, CH_2), 35.6 (d, $J_{C-P} = 4.6 \text{ Hz}$, C), 30.1 (d, $J_{C-P} = 5.6 \text{ Hz}$, 3 × CH₃), 26.6 (CH₃), 23.8 (CH₃), 23.0 (CH₃), 16.5 (d, $J_{C-P} = 5.8$ Hz, CH₃), 16.2 (d, $J_{\text{C-P}} = 6.6 \text{ Hz}$, CH₃). HRMS m/z (ESI) Calcd for $C_{28}H_{45}NO_6P^+$ $[M + H]^+$ 522.2979 Found: 522.2977. (RS/SR)-4b; pale yellow oil; $R_{\rm f} = 0.74$ (EP/EtOAc 7:3); ¹H NMR (400 MHz, CDCl₃) δ 7.38-7.16 (m, 5H), 7.26 (d, J = 8.6 Hz, 2H), 6.82 (d, J = 8.7 Hz, 2H), 5.01 (q, J = 6.5 Hz, 1H), 4.94 (s, 2H), 4.48 (s, 1H), 3.90-3.51 (m, 5H), 3.71 (d, $J_{H-P} = 27.2$ Hz, 1H), 3.44 (d, J = 12.2Hz, 1H), 1.44 (d, J = 6.6 Hz, 3H), 1.17 (s, 3H), 1.11–1.03 (m, 15H), 1.00 (t, J = 7.0 Hz, 3H). ³¹P NMR (121 MHz, CDCl₃) δ 26.61. 13 C NMR (101 MHz, CDCl3) δ 157.7 (C), 137.0 (C), 135.84 (C), 128.4 (2 × CH), 127.7 (CH), 127.7 (2 × CH), 127.3 $(2 \times CH)$, 114.3 $(2 \times CH)$, 77.6 (CH), 69.8 (CH_2) , 69.6 $(d, J_{C-P} =$ 136.4 Hz, CH), 67.8 (CH₂), 64.5 (C), 61.9 (d, J_{C-P} = 6.5 Hz, CH₂), 60.3 (d, J_{C-P} = 7.8 Hz, CH₂), 35.2 (d, J_{C-P} = 4.2 Hz, C), 30.5 (d, $J_{C-P} = 5.7 \text{ Hz}, 3 \times \text{CH}_3$, 26.5 (d, $J_{C-P} = 75.2 \text{ Hz}, \text{CH}_3$), 24.0 (CH_3) , 21.7 (CH_3) , 16.2 $(d, J_{C-P} = 5.6 \text{ Hz}, CH_3)$, 15.9 $(d, J_{C-P} =$ 6.6 Hz, CH₃). HRMS m/z (ESI) Calcd for $C_{28}H_{45}NO_6P^+$ [M + H]⁺ 522.2979 Found: 522.2975.

Synthesis of O-(1-(4-(benzyloxy)phenyl)ethyl)-N,N-di-tertbutylhydroxylamine (5b). Alkoxyamines 5b was prepared according to the general procedure using Salen ligand (138 mg, 0.516 mmol, 0.15 eq.), MnCl₂ (102 mg, 0.516 mmol, 0.15 eq.), 5' (500 mg, 3.443 mmol, 1.0 eq.), 4-vinylbenzylphenol (869 mg, 4.131 mmol, 1.2 eq.) and NaBH₄ (651 mg, 17.215 mmol, 5.0 eq.). Alkoxyamine was purified by automatic flash column chromatography (petroleum ether/EtOAc; gradient: 100% to 80%) to afford 5b (709 mg, 58%), white solid; m.p.: 104 °C; $R_f = 0.63$ (EP/EtOAc 96:4); ¹H NMR (400 MHz, CDCl₃) δ 7.51–7.32 (m, 5H), 7.26 (d, J = 8.6 Hz, 2H), 6.94 (d, J = 8.6 Hz, 2H), 5.07 (s, 2H), 4.81 (q, J = 6.7 Hz, 1H), 1.49 (d, J = 6.7Hz, 3H), 1.32 (s, 9H), 1.05 (s, 9H). ¹³C NMR (101 MHz, CDCl₃) δ 157.8 (C), 137.7 (C), 137.2 (C), 128.5 (2 × CH), 128.2 (2 × CH), 127.8 (CH), 127.5 (2 × CH), 114.2 (2 × CH), 82.0 (CH), 70.0 (CH_2) , 61.8 (C), 61.7 (C), 30.6 $(6 \times CH_3)$, 22.3 (CH_3) . HRMS m/z(ESI) Calcd for $C_{23}H_{34}NO_2^+$ [M + H]⁺ 356.2584 Found: 356.2579.

Synthesis of 1-(1-(3-(benzyloxy)phenyl)ethoxy)-2,2,6,6-tetramethylpiperidine (1d). Alkoxyamines 1d was prepared according to the general procedure using Salen ligand (52 mg, 0.195 mmol, 0.15 eq.), MnCl₂ (40 mg, 0.195 mmol, 0.15 eq.), 1° (203 mg, 1.297 mmol, 1.0 eq.), 3-vinylbenzylphenol (300 mg, 1.426 mmol, 1.1 eq.) and NaBH₄ (245 mg, 6.485 mmol, 5.0 eq.). Alkoxyamine was purified by automatic flash column chromatography (petroleum ether/EtOAc; gradient: 100% to 80%) to afford **1d** (119 mg, 25%), white solid; m.p.: 101 °C; R_f = 0.75 (EP/EtOAc 96:4); 1 H NMR (400 MHz, CDCl₃) δ 7.37 (m, 2H), 7.28 (m, 3H), 7.14 (m, 1H), 6.89 (m, 1H), 6.83 (m, 1H), 6.77 (m, 1H), 4.99 (s, 2H), 4.67 (q, J = 6.6 Hz, 1H), 1.40 (m, 6H), 1.38 (d, J = 6.7 Hz, 3H), 1.20 (s, 3H), 1.08 (s, 3H), 0.94 (s, 3H), 0.62 (s, 3H). 13 C NMR (101 MHz, CDCl₃) δ 158.7 (C), 147.6 (C), 137.2 (C), 129.0 (CH), 128.5 (2 × CH), 127.9 (CH), 127.6 (2 × CH), 119.3 (CH), 113.2 (CH), 113.1 (CH), 83.1 (CH), 70.0 (CH₂), 59.7 (2 × C), 40.4 (2 × CH₂), 34.5 (CH₃), 34.1 (CH₃), 23.6 (CH₃), 20.4 (2 \times CH₃), 17.2 (CH₂). HRMS m/z (ESI) Calcd for $C_{24}H_{34}NO_2^+[M+H]^+$ 368.2584 Found: 368.2588.

Synthesis diethyl(1-((1-(3-(benzyloxy)phenyl)ethoxy) of (tert-butyl)amino)-2,2-dimethylpropyl)phosphonate (3d).Alkoxyamines 3d was prepared according to the general procedure using Salen ligand (69 mg, 0.259 mmol, 0.15 eq.), MnCl₂ (51 mg, 0.259 mmol, 0.15 eq.), 3° (504 mg, 1.729 mmol, 1.0 eq.), 3-vinylbenzylphenol (400 mg, 1.902 mmol, 1.1 eq.) and NaBH₄ (196 mg, 5.187 mmol, 3.0 eq.). The solvent was evaporated to give the crude product as mixture of diastereoisomers. The diastereoisomers were separated by automatic flash column chromatography (petroleum ether/EtOAc; gradient: 100% to 50%) to afford (RR/SS)-3d (245 mg, 28%) and (RS/ SR)-3d (235 mg, 27%). (RR/SS)-3d; pale yellow oil; $R_f = 0.54$ (EP/ EtOAc 4:1); ¹H NMR (400 MHz, CDCl₃) δ 7.38 (m, 5H), 7.22 (t, J = 7.8 Hz, 1H, 6.91 (m, 2H), 6.85 (m, 1H), 5.07 (s, 2H), 4.96 (q, 2H)J = 6.7 Hz, 1H, 4.35 (m, 1H), 4.10 (m, 2H), 3.98 (m, 1H), 3.34 $(d, J_{H-P} = 26.1 \text{ Hz}, 1H), 1.59 (d, J = 6.8 \text{ Hz}, 3H), 1.34 (t, J = 7.1)$ Hz, 3H), 1.31 (t, J = 7.1 Hz, 3H), 1.24 (s, 9H), 0.85 (s, 9H). ³¹P NMR (121 MHz, CDCl₃) δ 25.91. ¹³C NMR (101 MHz, CDCl₃) δ 158.6 (C), 147.3 (C), 137.1 (C), 129.0 (CH), 128.6 (2 × CH), 127.9 (CH), 127.4 (2 × CH), 119.9 (CH), 113.8 (CH), 113.5 (CH), 85.5 (CH), 69.9 (CH₂), 69.9 (d, J_{C-P} = 138.5 Hz, CH), 61.6 (d, $J_{C-P} = 6.3 \text{ Hz}, CH_2$, 61.2 5 (C), 58.8 (d, $J_{C-P} = 7.5 \text{ Hz}, CH_2$), 35.6 (d, J_{C-P} = 5.8 Hz, C), 30.1 (d, J_{C-P} = 5.8 Hz, 3 × CH₃), 28.5 (3 × CH₃), 24.1 (CH₃), 16.8 (d, $J_{C-P} = 5.5$ Hz, CH₃), 16.3 (d, $J_{C-P} =$ 6.7 Hz, CH₃). HRMS m/z (ESI) Calcd for $C_{28}H_{45}NO_5P^+$ [M + H]⁺ 506.3030 Found: 506.3033. (RS/SR)-3d; pale yellow oil; $R_f = 0.67$ (EP/EtOAc 4:1); 1 H NMR (300 MHz, CDCl₃) δ 7.38 (m, 5H), 7.19 (t, J = 7.8 Hz, 1H), 7.08 (m, 2H), 6.85 (m, 1H), 5.22 (q, J =6.5 Hz, 1H), 5.07 (m, 2H), 3.91 (m, 2H), 3.45 (m, 1H), 3.40 (d, J_{H-P} = 26.1 Hz, 1H), 3.29 (m, 1H), 1.54 (d, J = 6.6 Hz, 3H), 1.24 (m, 6H), 1.21 (s, 9H), 1.19 (s, 9H), 0.91 (t, J = 7.1 Hz, 3H). ³¹P NMR (121 MHz, CDCl₃) δ 24.65. ¹³C NMR (75 MHz, CDCl₃) δ 158.5 (C), 145.1 (C), 137.3 (C), 128.9 (CH), 128.5 (2 × CH), 127.8 (2 × CH), 127.4 (CH), 120.8 (CH), 114.1 (CH), 113.9 (CH), 78.2 (CH), 70.1 (CH₂), 70.0 (d, J_{C-P} = 139.1 Hz, CH), 61.6 (d, $J_{C-P} = 6.4 \text{ Hz}$, CH_2), 61.3 (C), 58.7 (d, $J_{C-P} = 7.5 \text{ Hz}$, CH_2), 35.4 $(d, J_{C-P} = 5.1 \text{ Hz}, C), 30.7 (d, J_{C-P} = 6.0 \text{ Hz}, 3 \times CH_3), 28.3 (3 \times CH_3)$

 CH_3), 21.3 (CH_3), 16.4 (d, $J_{C-P} = 5.7$ Hz, CH_3), 16.2 (d, $J_{C-P} = 6.9$ Hz, CH₃). HRMS m/z (ESI) Calcd for $C_{28}H_{45}NO_5P^+$ [M + H]⁺ 506.3030 Found: 506.3032.

4-(1-((2,2,6,6-tetramethylpiperidin-1-yl)oxy) **Synthesis** of ethyl)phenol (1a). Alkoxyamines 1a was prepared according to the general procedure of hydrogenation using benzylated alkoxyamine 1b (300 mg, 0.544 mmol, 1 eq.) Alkoxyamine was purified by automatic flash column chromatography (petroleum ether/EtOAc; gradient: 100% to 60%) to afford 1a (86 mg, 57%), pale orange oil; $R_f = 0.63$ (EP/EtOAc 4:1); ¹H NMR (400 MHz, CDCl3) δ 7.11 (d, J = 7.7 Hz, 2H), 6.71 (d, J = 7.8 Hz, 2H), 4.65 (q, J = 6.7 Hz, 1H), 1.38 (d, J = 6.7 Hz, 3H), 1.56-0.84 (m, 15H), 0.58 (s, 3H). ¹³C NMR (75 MHz, CDCl₃) δ 154.5 (C), 136.8 (C), 127.4 (2 × CH), 114.6 (2 × CH), 81.8 (CH), 59.0 (2 × C), 39.7 (2 × CH₂), 33.6 (2 × CH₃), 22.5 (CH₃), 19.7 (2 × CH₃), 16.6 (CH₂). HRMS m/z (ESI) Calcd for $C_{17}H_{28}NO_2^{-1}$ $[M + H]^{+}$ 278.2115 Found: 278.2115.

Synthesis of 4-(1-((2,2,5,5-tetramethylpyrrolidin-1-yl)oxy) ethyl)phenol (2a). Alkoxyamines 2a was prepared according to the general procedure of hydrogenation using benzylated alkoxyamine 2b (200 mg, 0.566 mmol, 1 eq.) Alkoxyamine was purified by automatic flash column chromatography (petroleum ether/EtOAc; gradient: 100% to 60%) to afford 2a (120 mg, 81%), white solid; m.p.: 62 °C; $R_f = 0.73$ (EP/EtOAc 4:1); ¹H NMR (400 MHz, CDCl₃) δ 7.22 (d, J = 7.4 Hz, 2H), 6.78 (d, J = 8.0 Hz, 2H), 4.60 (q, J = 6.7 Hz, 1H), 1.56 (s, 3H), 1.45(m, 1H), 1.44 (d, J = 6.6 Hz, 3H), 1.25 (s, 3H), 1.15 (s, 3H), 1.02(s, 3H), 0.67 (s, 3H). 13 C NMR (75 MHz, CDCl₃) δ 154.4 (C), 137.1 (C), 128.3 (2 × CH), 115.3 (2 × CH), 81.5 (CH), 64.1 (C), 63.0 (C), 35.9 (CH₂), 35.2 (CH₂), 31.0 (CH₃), 30.9 (CH₃), 24.1 (CH₃), 22.7 (CH₃), 21.9 (CH₃). HRMS m/z (ESI) Calcd for $C_{16}H_{25}NO_2^+[M+H]^+$ 264.1958 Found: 264.1956.

Synthesis of diethyl (1-(*tert*-butyl(1-(4-hydroxyphenyl)ethoxy) amino)-2,2-dimethylpropyl)phosphonate (3a). Alkoxyamines (RR/SS)-3a or (RS/SR)-3a was prepared according to the general procedure of hydrogenation using benzylated alkoxyamine (RR/SS)-3b (200 mg, 0.396 mmol, 1 eq.) or (RS/SR)-3b (200 mg, 0.396 mmol, 1 eq.) Alkoxyamines were purified by automatic flash column chromatography (petroleum ether/EtOAc; gradient: 100% to 40%) to afford (RR/SS)-3a (125 mg, 76%) or (RR/ SS)-3a (118 mg, 72%). (RR/SS)-3a: white solid m.p.: 115 °C (decomp.); $R_f = 0.50$ (EP/EtOAc 3:2); ¹H NMR (400 MHz, $CDCl_3$) δ 7.14 (d, J = 7.3 Hz, 2H), 6.86 (d, J = 8.5 Hz, 2H), 4.93 (q, J = 6.6 Hz, 1H), 4.37-4.18 (m, 1H), 4.19-3.89 (m, 3H), 3.37 $(d, J_{H-P} = 26.4 \text{ Hz}, 1\text{H}), 1.58 (d, J = 6.6 \text{ Hz}, 3\text{H}), 1.29 (m, 6\text{H}),$ 1.25 (s, 9H), 0.88 (s, 9H). ³¹P NMR (121 MHz, CDCl₃) δ 25.88. 13 C NMR (75 MHz, CDCl₃) δ 156.3 (C), 135.9 (C), 128.4 (2 \times CH), 115.0 (2 × CH), 84.3 (CH), 70.0 (d, J_{C-P} = 139.1 Hz, CH), 61.9 (d, $J_{C-P} = 6.3$ Hz, CH_2), 61.3 (C), 59.3 (d, $J_{C-P} = 7.8$ Hz, CH_2), 35.6 (d, J_{C-P} = 5.5 Hz, C), 30.2 (d, J_{C-P} = 5.9 Hz, 3 × CH_3), 28.5 (3 × CH₃), 23.5 (CH₃), 16.5 (d, J_{C-P} = 5.9 Hz, CH₃), 16.2 (d, $J_{\text{C-P}} = 7.1 \text{ Hz}$, CH₃). HRMS m/z (ESI) Calcd for $C_{21}H_{39}NO_5P^+$ $[M + H]^+$ 416.2560 Found: 416.2560. (RS/SR)-3a: white solid m.p.: 115 °C (decomp.); $R_f = 0.70$ (EP/EtOAc 3:2); ¹H NMR (400 MHz, CDCl₃) δ 7.18 (d, J = 8.5 Hz, 2H), 6.74 (d, J = 8.5 Hz, 2H), 5.17 (q, J = 6.5 Hz, 1H), 4.18–3.70 (m, 3H), 3.50–3.45 (m,

1H), 3.47 (d, J_{H-P} = 26.6 Hz, 1H), 1.52 (d, J = 6.6 Hz, 3H), 1.23 (d, J = 2.4 Hz, 21H), 0.98 (t, J = 7.1 Hz, 3H). ³¹P NMR (121 MHz, CDCl₃) δ 25.05. ¹³C NMR (75 MHz, CDCl₃) δ 156.9 (C), 133.6 (C), 128.7 (2 × CH), 115.2 (2 × CH), 78.5 (CH), 70.5 (d, J_{C-P} = 139.7 Hz, CH), 62.5 (d, J_{C-P} = 6.6 Hz, CH₂), 61.2 (C), 59.1 (d, $J_{\text{C-P}} = 7.5 \text{ Hz}, \text{ CH}_2$, 35.4 (d, $J_{\text{C-P}} = 5.2 \text{ Hz}, \text{ C}$), 30.8 (d, $J_{\text{C-P}} =$ 6.1 Hz, $3 \times \text{CH}_3$), 28.3 (3 × CH₃), 21.6 (CH₃), 16.4 (d, $J_{\text{C-P}}$ = 5.7 Hz, CH₃), 16.1 (d, $J_{C-P} = 7.1$ Hz, CH₃). HRMS m/z (ESI) Calcd for $C_{21}H_{39}NO_5P^+[M+H]^+$ 416.2560 Found: 416.2558.

Research Article

Synthesis of diethyl(1-((1-hydroxy-2-methylpropan-2-yl)(1-(4hydroxyphenyl)ethoxy)amino)-2,2 dimethylpropyl)phosphonate (4a). Alkoxyamines (RR/SS)-4a or (RS/SR)-4a was prepared according to the general procedure of hydrogenation using benzylated alkoxyamine (RR/SS)-4b (200 mg, 0.373 mmol, 1 eq.) and (RS/SR)-4b (300 mg, 0.560 mmol, 1 eq.) Alkoxyamines were purified by automatic flash column chromatography (petroleum ether/EtOAc; gradient: 100% to 40%) to afford (RR/SS)-4a (127 mg, 79%) or (RR/SS)-4a (185 mg, 77%). (RR/SS)-4a: white solid m.p.: 115 °C (decomp.); $R_f = 0.30$ (EP/ EtOAc 1:1); ¹H NMR (400 MHz, CDCl₃) δ 7.12 (d, J = 8.0 Hz, 2H), 6.75 (d, J = 8.2 Hz, 2H), 4.80 (q, J = 6.5 Hz, 1H), 4.37–3.91 (m, 5H), 3.55 (d, J_{H-P} = 26.6 Hz, 1H), 3.39 (d, J = 12.1 Hz, 1H), 3.10 (d, J = 12.1 Hz, 1H), 1.46 (d, J = 6.6 Hz, 2H), 1.27 (m, 6H),1.15 (s, 9H), 0.97 (s, 3H), 0.78 (s, 3H). ³¹P NMR (162 MHz, CDCl₃) δ 27.06. ¹³C NMR (101 MHz, CDCl₃) δ 156.5 (C), 135.5 (C), 127.9 (2 × CH), 115.2 (2 × CH), 84.5 (CH), 69.6 (d, J_{C-P} = 136.4 Hz, CH), 67.4 (CH₂), 64.8 (C), 62.0 (d, J_{C-P} = 6.6 Hz, CH₂), 60.8 (d, J_{C-P} = 8.0 Hz, CH₂), 35.7 (d, J_{C-P} = 4.5 Hz, C), 30.1 (d, $J_{C-P} = 5.6 \text{ Hz}, 3 \times \text{CH}_3$, 26.8 (CH₃), 24.1 (CH₃), 23.2 (CH₃), 16.5 $(d, J_{C-P} = 5.8 \text{ Hz}, CH_3), 16.2 (d, J_{C-P} = 6.8 \text{ Hz}, CH_3). (RS/SR)-4a$: white solid m.p.: 115 °C (decomp.); $R_f = 0.45$ (EP/EtOAc 1:1); ¹H NMR (400 MHz, CDCl₃) δ 9.01 (s, 1H), 7.24 (d, J = 8.1 Hz, 2H), 6.79 (d, J = 8.2 Hz, 2H), 5.11 (q, J = 6.5 Hz, 1H), 4.51 (s, 1H), 4.01–3.64 (m, 6H), 3.79 (d, J_{H-P} = 26.6 Hz, 1H), 1.55 (d, J = 6.5 Hz, 3H), 1.33 (s, 3H), 1.28-1.04 (m, 18H). ³¹P NMR (162 MHz, CDCl₃) δ 26.30. ¹³C NMR (101 MHz, CDCl₃) δ 156.7 (C), 133.6 (C), 127.8 (2 × CH), 115.1 (2 × CH), 78.2 (CH), 70.1 $(d, J_{C-P} = 136.7 \text{ Hz}, CH), 68.2 (CH₂), 64.4 (C), 62.5 (d, <math>J_{C-P} = 6.6$ Hz, CH₂), 60.7 (d, J_{C-P} = 8.0 Hz, CH₂), 35.4 (d, J_{C-P} = 4.4 Hz, C), 30.5 (d, J_{C-P} = 5.8 Hz3 × CH₃), 26.2 (CH₃), 23.9 (CH₃), 21.7 (CH_3) , 16.3 $(d, J_{C-P} = 5.8 \text{ Hz}, CH_3)$, 16.0 $(d, J_{C-P} = 6.9 \text{ Hz}, CH_3)$. HRMS m/z (ESI) Calcd for $C_{21}H_{39}NO_6P^+$ [M + H]⁺ 432.2510 Found: 432.2507 (for a mixture of diastereoisomers).

Synthesis of 4-(1-((di-tert-butylamino)oxy)ethyl)phenol (5a). Alkoxyamines 5a was prepared according to the general procedure of hydrogenation using benzylated alkoxyamine 5b (250 mg, 0.703 mmol, 1 eq.) Alkoxyamine was purified by automatic flash column chromatography (petroleum ether/EtOAc; gradient: 100% to 60%) to afford 5a (91 mg, 49%), pale orange oil; $R_f = 0.58$ (EP/EtOAc 4:1); HRMS m/z (ESI) Calcd for $C_{16}H_{28}NO_2^+[M+H]^+$ 266.2115 Found: 266.2114.

Synthesis of diethyl (1-(tert-butyl(1-(3-hydroxyphenyl)ethoxy) amino)-2,2-dimethylpropyl)phosphonate (3e). Alkoxyamines (RR/SS)-3e or (RS/SR)-3e was prepared according to the general procedure of hydrogenation using benzylated alkoxyamine (RR/SS)-3d (90 mg, 0.178 mmol, 1 eq.) or (RS/SR)-3d (150 mg,

0.297 mmol, 1 eq.) Alkoxyamines were purified by automatic flash column chromatography (petroleum ether/EtOAc; gradient: 100% to 40%) to afford (RR/SS)-3e (53 mg, 71%) or (RR/ SS)-3e (95 mg, 77%). (RR/SS)-3e: white solid m.p.: 115 °C (decomp.); $R_f = 0.50$ (EP/EtOAc 3:2); ¹H NMR (400 MHz, CDCl₃) δ 8.31 (s, 1H), 7.04 (t, J = 7.7 Hz, 1H), 6.83 (s, 1H), 6.71 (t, J = 7.1 Hz, 2H), 4.85 (q, J = 6.5 Hz, 1H), 4.25 (m, 1H), 4.00(m, 3H), 3.30 (d, J_{H-P} = 26.1 Hz, 1H), 1.50 (d, J = 6.7 Hz, 3H), 1.23 (m, 6H), 1.17 (s, 9H), 0.83 (s, 9H). ³¹P NMR (121 MHz, CDCl₃) δ 26.14. ¹³C NMR (101 MHz, CDCl₃) δ 156.8 (C), 146.8 (C), 129.0 (CH), 118.3 (CH), 114.2 (CH), 114.2 (CH), 85.5 (CH), 70.0 (d, J_{C-P} = 138.7 Hz, CH), 62.1 (d, J_{C-P} = 6.4 Hz, CH₂), 61.4 (C), 59.3 (d, $J_{C-P} = 7.5$ Hz, CH₂), 35.7 (d, $J_{C-P} = 5.7$ Hz, C), 30.0 $(d, J_{C-P} = 5.7 \text{ Hz}, 3 \times CH_3), 28.6 (3 \times CH_3), 24.2 (CH_3), 16.7 (d, 3.4)$ $J_{\text{C-P}} = 5.6 \text{ Hz}, \text{ CH}_3$), 16.2 (d, $J_{\text{C-P}} = 6.9 \text{ Hz}, \text{ CH}_3$). HRMS m/z(ESI) Calcd for $C_{21}H_{39}NO_5P^+$ [M + H]⁺ 416.2560 Found: 416.2562. (RS/SR)-3e: white solid m.p.: 115 °C (decomp.); $R_f =$ 0.70 (EP/EtOAc 3:2); 1 H NMR (400 MHz, CDCl₃) δ 1 H NMR (400 MHz, CDCl₃) δ 8.73 (s, 1H), 7.10 (t, J = 7.8 Hz, 1H), 7.03 (s, 1H), 6.94 (d, J = 7.6 Hz, 1H), 6.74 (dd, J = 8.0, 1.6 Hz, 2H), 5.17 $(q, J = 6.5 \text{ Hz}, 1\text{H}), 3.91 \text{ (m, 2H)}, 3.56 \text{ (m, 2H)}, 3.44 \text{ (d, } J_{H-P} =$ 26.3 Hz, 1H), 1.53 (d, J = 6.5 Hz, 3H), 1.22 (m, 21H), 0.97 (t, J =7.1 Hz, 3H). ³¹P NMR (121 MHz, CDCl₃) δ 24.97 ¹³C NMR (101 MHz, CDCl₃) δ 156.9 (C), 144.7 (C), 128.9 (CH), 117.9 (CH), 115.3 (CH), 114.5 (CH), 78.7 (CH), 70.3 (d, J = 139.5 Hz, CH), 62.4 (d, J = 6.5 Hz, CH₂), 61.4 (C), 59.1 (d, J = 7.6 Hz, CH_2), 35.5 (d, J = 5.1 Hz, C), 30.6 (d, J = 6.0 Hz, $3 \times CH_3$), 28.3 $(3 \times CH_3)$, 21.66 (CH₃), 16.40 (d, J = 5.8 Hz, CH₃), 16.08 (d, J =7.2 Hz, CH₃). HRMS m/z (ESI) Calcd for $C_{21}H_{39}NO_5P^+$ [M + H]⁺ 416.2560 Found: 416.2561.

Chemical oxidation as trigger

Addition of several equivalents of lead dioxide PbO2 to a 0.1 mM solution of alkoxyamines 1a-5a, and after a vigorous 20 seconds hand-shaking, provides an EPR signal. Then, using this procedure, effect of 10 equivalents to 1500 equivalents of PbO₂ on alkoxyamines 1a-5a was tested (ESI Table 1†). Nitroxides 4° and 5° are not stable in the presence of PbO₂, presumably due to further oxidation to oxoamoniums, impeding the growth of significant EPR signals upon oxidation of the corresponding alkoxyamines (only a few percent of conversion were detected). For low amounts of PbO2, more vigorous handshakings do not increase the amount of released nitroxide.

CIDNP experiments

¹H NMR and CIDNP spectra were recorded on a 200 MHz Bruker AVANCE DPX spectrometer. In situ irradiation of samples inside NMR magnet was carried out by using a frequency-tripled Quantel Brilliant B Nd:YAG laser (355 nm, 8 ns, ca. 70 mJ per pulse) The following pulse sequence was used: presaturation (laser flash)-(RF)-(detection pulse, 2 us)-(free induction decay). Dark spectra (without the laser flash) were always recorded as a reference for a proper suppression of the background NMR transitions.

Deuterated solvents were purchased from Sigma-Aldrich and used without additional treatment. All the samples were

deaerated by bubbling with N2 for 5 minutes prior to the CIDNP experiment.

DFT calculations

All calculations were performed using the Gaussian 16 electronic structure package⁵⁵ at the M06-2X/6-31+G(d,p) level of theory,⁵³ and the nature of all stationary points confirmed with frequency calculations at the same level. Gas-phase Gibbs free energies at 298.15 K were calculated using standard textbook formulae based upon the statistical thermodynamics of an ideal gas under the harmonic oscillator and rigid-rotor approximations. Solvent corrections were obtained with the SMD continuum solvent model for methanol,⁵⁶ and the thermocycle approach was employed to determine Gibbs free energies in solution.⁵⁷ All energies given are from conformation-Boltzmann-weighted ally-searched distributions.

HPLC measurements and mass spectral analyses

Alkoxyamines and their homolysed products were separated and monitored by HPLC using an Agilent 1260 apparatus equipped with a UV-Vis absorption and MS detector. Typically, 1 μl of a sample was injected on C18 column (Phenomenex, Luna Omega Polar 1.6 µm, 100 × 2.1 mm) equilibrated with acetonitrile/water mobile phase (15/85 v/v) containing 0.1% formic acid. Compounds were separated by a linear increased of the acetonitrile concentration from 15 to 100% over 8 min. Next, the concentration of acetonitrile was kept at this level for 13 min. All analytes, were eluted at a flow rate of 0.14 ml min⁻¹. The absorption traces were collected at 230 nm. The structural identity of products was confirmed by MS analysis using an Agilent 6120 quadrupole mass spectrometer equipped with electrospray ion source. The compounds were detected in the positive-ion mode.

Kinetic measurements

Rate constants k_d for the homolysis of the C-ON bond of alkoxyamines 1a,b-5a,b (Scheme 7) are determined using eqn (2) and by monitoring the growth of nitroxide by EPR, using O₂ as alkyl radical scavenger as previously reported.⁵⁸ For all alkoxyamines, a plateau in nitroxides is reached for more than 90% conversion at any temperatures. For the sake of simplicity, activation energies E_a are estimated using the Arrhenius equation in conjunction with the averaged frequency factor A =2.4 10^{14} s⁻¹. For ease of discussion, values of k'_d at 120 °C are obtained from the Arrhenius equation, and half lives $(t_{1/2})$

$$R_1$$
 $N-O$
 R_2
 t -BuPh
 R_2
 R_1
 $N-O$
 t
+ oxidation products
 R_2
 R_2
 R_2
 R_2

Scheme 7 Thermal homolysis of 1a,b-5a,b in t-BuPh in the presence of O2 as scavenger at various temperatures.

are obtained assuming first order kinetics. All data are gathered in Table 1.

$$\ln \frac{[\text{nitroxide}]_{\infty} - [\text{nitroxide}]_{t}}{[\text{nitroxide}]_{\infty}} = -k_{d} \cdot t \tag{2}$$

Conclusions

Oxidation of bench stable alkoxyamines yields highly reactive intermediates capable of undergoing S_N2 reactions with nucleophiles and/or mesolytic cleavage to form carbon-centred radicals or carbocations for use in chemical synthesis. To date electrochemical and photoredox methods have been used for this purpose; in this contribution we show that chemical oxidation provides a mild and convenient alternative. Moreover, when the nitroxide bears phenolic leaving groups we show that alkoxyamine cleavage can also be triggered by proton coupled electron transfer followed by a β-fragmentation reaction to afford methine quinone like-compounds. Both processes have potential to expand the scope of smart alkoxyamines in chemical synthesis, and as reporter molecules of oxidising environments.

Author contributions

All authors contribute equally.

Conflicts of interest

There are no conflicts to declare.

Acknowledgements

SRAM, MH and GA are thankful to Aix-Marseille University and CNRS for support. JH and MH are grateful to ANR for support (ANR-17-CE18-0017 and ANR-15-CE18-0012-01). SJ and EV thank Ministry for support. TMMK thank Campus France and government of Gabon for support. MLC gratefully acknowledges generous allocations of supercomputing time on the National Facility of the National Computational Infrastructure and an Australian Research Council Laureate Fellowship (FL170100041).

Notes and references

- 1 G. Audran, P. Brémond, J.-M. Franconi, S. R. A. Marque, P. Massot, P. Mellet, E. Parzy and E. Thiaudière, Alkoxyamines: a New Family of Pro-Drugs against Cancer. Concept for Theranostics, Org. Biomol. Chem., 2014, 12, 719.
- 2 P. Brémond, A. Koïta, S. R. A. Marque, V. Pesce, V. Roubaud and D. Siri, Chemically Trigerred C—ON Bond Homolysis of

- Alkoxyamines. Quaternization of the Alkyl Fragments, Org. Lett., 2012, 14(1), 358.
- 3 G. Audran, E. Bagryanskaya, I. Bagryanskaya, P. Brémond, M. Edeleva, S. R. A. Marque, D. Parkhomenko, E. Tretyakov and S. Zhivetyeva, C-ON Bond Homolysis of Alkoxyamines Triggered by Paramagnetic Copper(II) Salts, Inorg. Chem. Front., 2016, 3(11), 1464.
- 4 G. Gryn'ova, D. L. Marshall, S. J. Blanksby and M. L. Coote, Switching Radical Stability by pH-Induced Orbital Conversion, Nat. Chem., 2013, 5, 474.
- 5 G. Gryn'ova, L. M. Smith and M. L. Coote, Computational design of pH-switchable control agents for nitroxide mediated polymerization, Phys. Chem. Chem. Phys., 2017, 19, 22678-22683.
- 6 Y. Guillaneuf, D.-L. Versace, D. Bertin, J. Lalevée, D. Gigmes and J.-P. Fouassier, Importance of the Position of the Chromophore Group on the Dissociation Process of Light Sensitive Alkoxyamine, Macromol. Rapid Commun., 2010, 31, 1909-1913.
- 7 Y. Guillaneuf, D. Bertin, D. Gigmes, D.-L. Versace, J. Lalevée and J.-P. Fouassier, Toward Nitroxide-Mediated Photopolymerization, Macromolecules, 2010, 43, 2204.
- 8 J. Morris, S. Telitel, K. E. Fairfull-Smith, S. E. Bottle, J. Lalevée, J.-L. Clément, Y. Guillaneuf and D. Gigmes, Novel polymer synthesis methodologies using combinations of thermally- and photochemically-induced nitroxide Mediated Polymerization, Polym. Chem., 2015, 6, 754-763
- 9 S. E. Bottle, J.-L. Clement, M. Fleige, E. M. Simpson, Y. Guillaneuf, K. E. Fairfull-Smith, D. Gigmes and J. P. Blinco, Light-Active Azaphenalene Alkoxyamines: Fast and Efficient Mediators of a Photo-Induced Persistent Radical Effect, RSC Adv., 2016, 6, 80328-80333.
- 10 G. Audran, L. Bosco, P. Brémond, N. Jugniot, S. R. A. Marque, P. Massot, P. Mellet, T. Moussounda Moussounda Koumba, E. Parzy, A. Rivot, E. Thiaudière, P. Voisin, C. Wedl and T. Yamasaki, Controlled Radical Initiation Triggered by Specific Enzymatic Activity, Org. Chem. Front., 2019, 6, 3663.
- 11 M. Albalat, G. Audran, M. Holzritter, S. R. A. Marque, P. Mellet, N. Vanthuyne and P. Voisin, An Enzymatic Acetal/Hemiacetal Conversion for the Physiological Temperature Activation of the Alkoxyamine C—ON Bond Homolysis, Org. Chem. Front., 2020, 7, 2916.
- 12 M. Edeleva, D. Morozov, D. Parkhomenko, Y. Polienko, A. Iurchenkova, I. Kirilyuk and E. G. Bagryanskaya, Versatile approach to activation of alkoxyamine homolysis by 1,3-dipolar cycloaddition for efficient and safe nitroxide mediated polymerization, Chem. Commun., 2019, 55, 190.
- 13 D. Moncelet, P. Voisin, N. Koonjoo, V. Bouchaud, P. Massot, E. Parzy, G. Audran, J.-M. Franconi, E. Thiaudière, S. R. A. Marque, P. Brémond and P. Mellet, Alkoxyamines: Towards a New Family of Theranostic Agents Against Cancer, Mol. Pharmaceutics, 2014, 11, 2412.
- 14 T. Yamasaki, D. Buric, Ch. Chacon, G. Audran, D. Braguer, S. R. A. Marque, M. Carré and P. Brémond, Chemical modi-

- fications of imidazole-containing alkoxyamines increase C-ON bond homolysis rate: effects on cytotoxic properties in glioblastoma cells, Bioorg. Med. Chem., 2019, 27, 1942.
- 15 A. Yamada, M. Abe, Y. Nishimura, S. Ishizaka, M. Namba, T. Nakashima, K. Shimoji and N. Hattori, Photochemical generation of the 2,2,6,6-tetramethylpiperidine-1-oxyl (TEMPO radical from, caged nitroxides by near-infrared two-photon irradiation and its cytocidal effect on lung cancer cells, Beilstein J. Org. Chem., 2019, 15, 863.
- 16 L. Tebben and A. Studer, Nitroxide: Applications in Synthesis and in Polymer Chemistry, Angew. Chem., Int. Ed., 2011, 50, 5034.
- E. Nutting, Rafiee 17 J. M. and S. S Stahl Tertamethylpiperidine N-oxyl (TEMPO)Phtalimide N-Oxyl (PINO), and Related N-Oxyl Species: Electrochemical Properties and Their Use in Electrocatalytic Reactions, Chem. Rev., 2018, 118, 4834.
- 18 T. Reyser, H. To, C. Egwu, L. Paloque, M. Nguyen, A. Hamouy, J.-L. Stigliani, C. Bijani, J.-M. Augereau, J.-P. Joly, J. Portela, J. Havot, S. R. A. Marque, J. Boissier, A. Robert, F. Benoit-Vical and G. Audran, Alkoxyamines Designed as Potential Drugs Against Plasmodium and Schistosoma Parasites, Molecules, 2020, e3838.
- 19 B. B. Noble, P. L. Norcott, C. L. Hammill, S. Ciampi and M. L. Coote, Mechanism of Oxidative Alkoxyamine Cleavage: the Surprising Role of the Solvent and Supporting Electrolyte, J. Phys. Chem. C, 2019, 123, 10300-10305.
- 20 C. L. Hammill, B. B. Noble, P. L. Norcott, S. Ciampi and M. L. Coote, Effect of Chemical Structure on the Electrochemical Cleavage of Alkoxyamines, J. Phys. Chem. C, 2019, **123**, 5273.
- 21 P. L. Norcott, C. L. Hammill, B. B. Noble, J. C. Robertson, A. Olding, A. C. Bissember and M. L. Coote, TEMPO-Me: an Electrochemically Activated Methylating Agent, J. Am. Chem. Soc., 2019, 141, 15450-15455.
- 22 F. J. M. Rogers, B. B. Noble and M. L. Coote, Computational optimization of alkoxyamine-based electrochemical methylation, J. Phys. Chem. A, 2020, 124, 6104-6110.
- 23 L. Zhang, E. Laborda, N. Darwish, B. B. Noble, J. H. Tyrell, S. Pluczyk, A. P. Le Brun, G. G. Wallace, J. Gonzalez, M. L. Coote and S. Ciampi, Electrochemical and Electrostatic Cleavage of Alkoxyamines, J. Am. Chem. Soc., 2018, 140, 766.
- 24 Q. Zhu, E. C. Gentry and R. R. Knowles, Catalytic nearbocation Generation Enabled nby the Mesolyticn Cleavage of Alkoxyamine radical Cation, Angew. Chem., Int. Ed., 2016, 55, 9969.
- 25 E. C. Gentry, L. J. Rono, M. E. Hale, R. Matsuura and Knowles, Enantioselective Synthesis Pyrroloindolines via Noncovalent Stabilization of Indole Radical Cations and Applications to the Synthesis of Alkaloid Natural Products, J. Am. Chem. Soc., 2018, 140(9), 3394.
- 26 N. S. Hill, M. J. Fule, J. Morris, J.-L. Clément, Y. Guillaneuf, D. Gigmes and M. L. Coote, Mesolytic versus homolytic

cleavage in photochemical nitroxide mediated polymerization, Macromolecules, 2020, 53, 1567-1572.

Organic Chemistry Frontiers

- 27 D. R. Weinberg, C. J. Gagliardi, J. F. Hull, C. F. Murphy, C. A. Kent, B. C. Westlake, A. Paul, D. H. Ess, D. G. McCafferty and T. J. Meyer, Proton-coupled electron transfer, Chem. Rev., 2012, 112, 4016.
- 28 J. B. Shotwell, E. S. Krygowski, J. Hines, B. Koh, E. W. D. Huntsman, H. W. Choi, J. S. Schneekloth Jr., J. L. Wood and C. M. Crews, Total synthesis of the antiangiogenic agent Luminacin D, Org. Lett., 2002, 18, 3087.
- 29 J. Dao, D. Benoît and C. J. Hawker, A Versatile and Efficient Synthesis of Alkoxyamine LFR Initiators via Manganese Based Asymmetric Epoxidation Catalysts, J. Polym. Sci., Part A: Polym. Chem., 1998, 36, 2161.
- 30 D. Bertin, D. Gigmes, S. R. A. Marque and P. Tordo, Polar, Steric, and Stabilization Effects in Alkoxyamines C-ON Bond Homolysis: Α Multiparameters Analysis, Macromolecules, 2005, 38(7), 2638.
- 31 H. Fischer, A. Kramer, S. R. A. Marque and P. Nesvadba, Steric and Polar Effects of the Cyclic Nitroxyl Fragment on the C-ON Bond Homolysis Rate Constant, Macromolecules, 2005, 38(24), 9974.
- 32 C. Y. Lin, S. R. A. Marque, K. Matyjaszewski and M. L. Coote, Linear-Free energy relationships for modeling structure-reactivity trends in Controlled Radical Polymerization, Macromolecules, 2011, 44(19), 7568-7583.
- 33 J. L. Hodgson, C.-Y. Lin, M. L. Coote, S. R. A. Marque and K. Matyjaszewski, Linear Free Energy Relationship for the Alkyl Affinities of Nitroxides: A Theoretical Study, Macromolecules, 2010, 43(8), 3728.
- 34 S. Marque, The influence of the nitroxide structure on homolysis rate of alkoxyamines: A Taft-Ingold analysis, J. Org. Chem., 2003, 68(20), 7582.
- 35 E. G. Bagryanskaya and S. R. A. Marque, Kinetic Aspects of Nitroxide-Mediated Polymerization, in Nitroxide Mediated Polymerization: From Fundamentals to Applications in Materials Sciences, RSC Polymer Chemistry Series, n° = 19, ed. D. Gigmes, Royal Society of Chemistry, 2016, ch. 2, pp. 45-113.
- 36 G. Gryn'ova, K. U. Ingold and M. L. Coote, New insights into the mechanism of amine/nitroxide cycling during the hindered amine light stabilizer inhibited oxidativen degradation of polymers, J. Am. Chem. Soc., 2012, 134, 12979-12988.
- 37 S. Marque, H. Fischer, E. Baier and A. Studer, Factors influencing the C-O-bond homolysis of alkoxyamines: Effect of H-bonding and polar substituents, J. Org. Chem., 2001, 66(4), 1146.
- 38 G. Audran, P. Brémond, J.-P. Joly, S. R. A. Marque and T. Yamasaki, C-ON bond homolysis of alkoxyamines. Part 12: Effect of the para-substituent in the 1-phenylethyl fragment, Org. Biomol. Chem., 2016, 14, 3574.
- 39 C. Hansch, A. Leo and R. W. Taft, A Survey of Hammett substituent constants and resonance and field parameters, Chem. Rev., 1991, 91, 165.
- 40 M. Charton, Adv. Mol. Struct. Res., 1999, 5, 25.

- 41 D. Bertin, D. Gigmes, S. R. A. Marque, S. Milardo, J. Peri and P. Tordo, Long-range polar effect on the C-ON bond homolysis in SG1 (N-(2-Methyl-2-propyl)-N-(1-diethylphosphono-2,2-dimethylpropyl)-N-oxyl) - alkoxyamines, Collect. Czech. Chem. Commun., 2004, 69(12), 2223.
- 42 G. Audran, S. Dorey, N. Dupuy, F. Gaston and S. R. A. Marque, Degradation of g-Irradiated Polyethyleneetylene Vinyl Alcohol-polyethylene Multilayer Films: An ESR Study, Polym. Degrad. Stab., 2015, 122, 169.
- 43 D. Griller and K. U. Ingold, Electron paramagnetic resonance and the art of physical-organic chemistry, Acc. Chem. Res., 1980, 13(7), 193.
- 44 J. J. Henderson, Concerning the relationship between the strength of acids and their capacity to preserve neutrality, Am. J. Physiol., 1908, 21, 173.
- 45 G. L. Closs and R. J. Miller, Gas-ohase basicities of amides and imidates. Estgim tion of protomeric equilibrium constants by the basicity method in the gas phase, J. Am. Chem. Soc., 1979, 101(6), 1639.
- 46 J.-K. Vollenweider, H. Fischer, J. Hennig and R. Leuschner, Time-resolved CIDNP in laser flash photolysis of aliphatic ketones. A quantitative analysis, Chem. Phys., 1985, 97(2-3), 217.
- 47 D. Neshchadin, F. Palumbo, M. S. Sinicropi, I. Andreu, G. Gescheidt and M. Miranda, Topological control in radical reactions of cholesterol in model dyads, Chem. Sci., 2013, 4(4), 1608.
- 48 I. Andreu, D. Neshchadin, S. N. Batchelor, M. A. Miranda and G. Gescheidt, Examples for biological reactivity involving free radicals followed by CIDNP, Mol. Phys., 2013, 111(18-19), 2992.
- 49 P. K. Das, M. V. Encinas, S. Steenken and J. C. Scaiano, Reaction of tert-butoxy radicals with phenols. Comparison with the reactions of carbon triplets, J. Am. Chem. Soc., 1981, 103(14), 4162.
- 50 M. V. Encinas and J. C. Scaiano, Reaction of Benzophznone triplets with allylic hydrogens. A laser flash photolysis study, J. Am. Chem. Soc., 1981, 103(21), 6393.
- 51 L. Hermosilla, J. M. G. de la Vega, C. Sieiro and P. Calle, DFT calculations of isotropic hyperfine couplking constants of nitrogen aromatic radicals: The challenge of nitroxide radicals, J. Chem. Theory Comput., 2011, 7(1), 169.
- 52 H. Kruse, L. Goerigk and S. W. Grimme, Why the standard B3LYP/6-31G* model chemistry should not be used in DFT calculations of molecular thermochemistry: Understanding and correcting the problem, J. Org. Chem., 2012, 77(23), 10824.
- 53 Y. Zhao and D. G. Truhlar, The M06 suite of density functional for main group thermochemistry, thermochemical kinetics, noncovalent interactions, excited states, and transition elements: Two new functional and systematic testing of four M06-class functional and 12 other functional, Theor. Chem. Acc., 2008, 120, 215.
- 54 J. W. Darcy, B. Koronkiewicz, G. A. Parada and J. M. Mayer, A continuum of proton-coupled electron transfer reactivity, Acc. Chem. Res., 2018, 51, 2391.

55 M. J. Frisch, G. W. Trucks, H. B. Schlegel, G. E. Scuseria, M. A. Robb, J. R. Cheeseman, G. Scalmani, V. Barone, G. A. Petersson, H. Nakatsuji, X. Li, M. Caricato, A. V. Marenich, J. Bloino, B. G. Janesko, R. Gomperts, B. Mennucci, H. P. Hratchian, J. V. Ortiz, A. F. Izmaylov, J. L. Sonnenberg, D. Williams-Young, F. Ding, F. Lipparini, F. Egidi, B. Goings, B. Peng, A. Petrone, T. Henderson, D. Ranasinghe, V. G. Zakrzewski, J. Gao, N. Rega, G. Zheng, W. Liang, M. Hada, M. Ehara, K. Toyota, R. Fukuda, J. Hasegawa, M. Ishida, T. Nakajima, Y. Honda, O. Kitao, H. Nakai, T. Vreven, K. Throssell, J. A. Montgomery Jr., J. E. Peralta, F. Ogliaro, M. J. Bearpark, J. J. Heyd, E. N. Brothers, K. N. Kudin, V. N. Staroverov, T. A. Keith, R. Kobayashi, J. Normand, K. Raghavachari, A. P. Rendell, J. C. Burant, S. S. Iyengar, J. Tomasi, M. Cossi,

Research Article

- J. M. Millam, M. Klene, C. Adamo, R. Cammi, J. W. Ochterski, R. L. Martin, K. Morokuma, O. Farkas, J. B. Foresman and D. J. Fox, Gaussian 16, revision C.01, Gaussian, Inc., Wallingford, CT, 2016.
- 56 A. V. Marenich, C. J. Cramer and D. G. Truhlar, Universal solvation model based on solute electron density and on continuum model of the solvent defined by the bulk dielectric constant a,d atomic surface tensions, J. Phys. Chem. B, 2009, 113, 6378.
- 57 J. Ho, A. Klamt and M. L. Coote, Comments on the correct use of continuum solvent models, J. Phys. Chem. A, 2010, 114, 13442.
- 58 S. Marque, C. Le Mercier, P. Tordo and H. Fischer, Factors influencing the C-O-bond homolysis of trialkylhydroxylamines, Macromolecules, 2000, 33(12), 4403.